Journal of Anatomy

J. Anat. (2020) **236**, pp668–687 doi: 10.1111/joa.13132

The iliosacral joint in lizards: an osteological and histological analysis

Ilaria Paparella[1] Aaron R. H. LeBlanc,[1] Michael R. Doschak[2] and Michael W. Caldwell[1,3]

[1]*Department of Biological Sciences, University of Alberta, Edmonton, AB, Canada*
[2]*Faculty of Pharmacy & Pharmaceutical Sciences and Department of Biomedical Engineering, University of Alberta, Edmonton, AB, Canada*
[3]*Department of Earth and Atmospheric Sciences, University of Alberta, Edmonton, AB, Canada*

Abstract

The development of the iliosacral joint (ISJ) in tetrapods represented a crucial step in the evolution of terrestrial locomotion. This structure is responsible for transferring forces between the vertebral column and appendicular skeleton, thus supporting the bodyweight on land. However, most research dealing with the water-to-land transition and biomechanical studies in general has focused exclusively on the articulation between the pelvic girdle and femur. Our knowledge about the contact between the pelvic girdle and vertebral column (i.e. the ISJ) at a tissue level is restricted so far to human anatomy, with little to no information available on other tetrapods. This lack of data limits our understanding of the development and evolution of such a key structure, and thus on the pattern and processes of the evolution of terrestrial locomotion. Therefore, we investigated the macro- and microanatomy of the ISJ in limb-bearing squamates that, similar to most non-mammalian, non-avian tetrapods, possess only two sacral ribs articulating with the posterior process of the ilium. Using a combination of osteology, micro-computed tomography and histology, we collected data on the ISJ apparatus of numerous specimens, sampling different taxa and different ontogenetic stages. Osteologically, we recorded consistent variability in all three processes of the ilium (preacetabular, supracetabular and posterior) and sacral ribs that correlate with posture and locomotion. The presence of a cavity between the ilium and sacral ribs, abundant articular cartilage and fibrocartilage, and a surrounding membrane of dense fibrous connective tissue allowed us to define this contact as a synovial joint. By comparison, the two sacral ribs are connected to each other mostly by dense fibrous tissue, with some cartilage found more distally along the margins of the two ribs, defining this joint as a combination of a syndesmosis and synchondrosis. Considering the intermediary position of the ISJ between the axial and appendicular skeletons, the shape of the articular surfaces of the sacral ribs and ilium, and the characteristics of the muscles associated with this structure, we argue that the mobility of the ISJ is primarily driven by the movements of the hindlimb during locomotion. We hypothesize that limited torsion of the ilium at the ISJ happens when the hip is abducted, and the joint is likely able to absorb the compressional and extensional forces related to the protraction and retraction of the femur. The mix of fibres and cartilage between the two sacral ribs instead serves primarily as a shock absorber, with the potential for limited vertical translation during locomotion.

Key words: cartilage ; comparative osteology ; diapophyses ; histology ; iliosacral joint ; joints; lymphapophyses; micro-computed tomography ; sacral ribs ; sacral vertebrae ; sacrum; squamata; synovial joint; transverse processes.

Introduction

In the water-to-land transition, a crucial change that made the *bauplän* of tetrapods suitable for terrestrial locomotion involves the establishment of an articulation between the pelvic girdle and the vertebral column via a sacral rib (Carroll et al. 2005). While most research has focused so far on the articulation between the pelvic girdle and the femur (i.e. the hip joint; Pierce et al. 2012; Arnold et al. 2014; Tsai & Holliday, 2015; Tsai et al. 2018), comparatively little attention has been given to the connection between the axial skeleton and the pelvic girdle in tetrapods. The iliosacral joint (ISJ) is the weight-bearing structure that transfers the force of gravity between the

Correspondence
Ilaria Paparella, Department of Biological Sciences, University of Alberta, Edmonton, AB T6G 2E9, Canada. E: paparell@ualberta.ca

Accepted for publication *14 November 2019*
Article published online *5 January 2020*

appendicular and axial skeletons (Wolff, 1990; Carroll et al. 2005). The axial component of the ISJ consists of modified vertebrae (sacrals) with elaborated ribs that extend to meet the pelvic girdle. In human anatomy, the sacrum is the single bony complex resulting from the fusion of sacral vertebrae located between the right and left pelves; however, the vertebrae may not fuse in other tetrapods (Gray, 1878; Romer, 1956; Hoffstetter & Gasc, 1969). The evolution of the ISJ allowed early tetrapods to shift towards hindlimb-powered locomotion (Coates et al. 2002; Boisvert, 2005). In amniotes, the ISJ consists of multiple rib-bearing sacral vertebrae attached to the ilium, increasing from the single vertebral attachment in early tetrapods; this evolutionary increase in the number of sacral vertebrae is probably correlated with changes in locomotory habits and lifestyle of terrestrial amniotes (Coates et al. 2002; Boisvert, 2005). For example, mammals, dinosaurs and birds can have more than two sacral vertebrae in contact with the pelvic girdle (Romer, 1956). In secondary aquatic amniotes instead, as a consequence of their 'return' to life in water, the ISJ is either reduced or lost – as in ichthyosaurs, mosasaurs and cetaceans (Gingerich et al. 1994; Motani et al. 1998; Bejder & Hall, 2002; Caldwell & Palci, 2007), or there is a significant increase in the number of sacral ribs contacting the ilium – as in plesiosaurs and nothosaurs (Cheng et al. 2004).

Most squamates, with the exclusion of limbless and obligatory aquatic forms, have two sacral vertebrae that articulate with the posterior process of the ilium (Snyder, 1954; Hoffstetter & Gasc, 1969; Caldwell & Palci, 2007). Moreover, instead of being completely fused together to form a sacrum, only the distal portions of the sacral ribs in squamates form a sutural contact with each other, whereas the vertebrae themselves are in most cases unfused (Hoffstetter & Gasc, 1969). Despite possessing a small number of unfused sacral vertebrae and a relatively slender ilium, the ISJ in squamates displays considerable variation in: (i) the positions of the sacral facets on the medial surface of the ilium (Borsuk-Białynicka, 2008); (ii) the orientation of the posterior iliac process in relation to the vertebral column (Borsuk-Białynicka, 2008); and (iii) the greater development of the supracetabular process of the ilium in facultatively bipedal lizards (Snyder, 1954). How this variation relates to muscle attachment, joint mobility, locomotory habits and phylogeny have not been explored in most amniotes. Considering the key role that the ISJ played in the colonization of the terrestrial environment by tetrapods (Carroll, 1988; Carroll et al. 2005), and the fact that squamates have been able to adapt to many different environments and locomotion styles, repeatedly evolving aquatic habits, bipedal posture or limblessness, we decided to characterize the anatomical details of this structure and to discuss its potential role in the evolutionary plasticity of this group.

Histological studies on the ISJ are not available for any amniote group, with the exception of humans (Forst et al. 2006; Rupert et al. 2009; Vleeming et al. 2012). Our study therefore aims to describe the ISJ in limb-bearing lizards, and to define the anatomical details of the elements involved in this structure (i.e. ilium and sacral ribs) using osteology, histology and micro-computed tomography (μCT).

Materials and methods

Specimens of iguanians were used to perform the histological analyses and μCT, whereas osteological comparisons are made across several groups of extant and fossil lizards in order to fully understand the complexity of this structure. A detailed list, with relative methodology applied to each specimen, is presented in Table 1. As different authors tend to use different terminology, especially when referring to the iliac processes, the anatomical nomenclature adopted in this study is illustrated in Fig. 1.

Specimens were scanned using a Bruker-SkyScan 1076 μCT scanner (Bruker-SkyScan, Kontich, Belgium) at the Pharmaceutical Orthopaedic Research Lab (University of Alberta). Samples were scanned at 18 μm resolution, with the cathode ray tube voltage/current set to 100 kV/100 μA, with low energy X-rays removed in all samples using a 1.0 mm aluminium filter. Three scan projections were averaged per step, through the 180° of rotation at 0.5° step increments with exposure times of 1180 ms for *Iguana iguana* UAMZ R951 and *Pogona vitticeps* UAMZ R952, and 885 ms for *Phrynosoma* sp. UAMZ R953. The two-dimensional raw image projections were reconstructed using a modified Feldkamp back-projection algorithm, with the cross-section to image conversion values set to 0.0–0.05 for *I. iguana* UAMZ R951 and *P. vitticeps* UAMZ R952, and 0.0–0.1 for *Phrynosoma* sp. UAMZ R953, using bundled vendor software (NRecon, version 1.7.0.4, Skyscan NV, Belgium). These settings allow for the capturing of bone and calcified cartilage, while unmineralized cartilage remains transparent. Three-dimensional reconstructions as well as additional two-dimensional images from the μCT scans were generated using Dragonfly [ver. 2.0 for Windows; Object Research Systems (ORS), Montreal, Canada, 2016].

Iguana iguana UAMZ R951 was μCT-scanned and then partially dissected, removing the skin and superficial musculature in order to extract the ISJ for serial histology. *Pogona vitticeps* UAMZ R952 was completely dissected after being μCT-scanned, in order to observe ligaments and muscle attachments, following Snyder (1954). *Phrynosoma* sp. UAMZ R953 was μCT-scanned and skeletonized. This specimen represents a subadult stage (incomplete skeletal maturity based on basicranial sutures) and shows evidence of partial mummification that caused the capturing of both unmineralized and mineralized cartilage during the scans (Panzer et al. 2015). This resulted in an usually thick cartilaginous layer at the distal end of the sacral ribs of UAMZ R953 (visible both in the scan frames and three-dimensional reconstructions). All the other specimens listed in Table 1 were used to collect anatomical data on the skeletal elements involved in the ISJ (i.e. pelvic girdle and sacral region of the column), looking at both articulated and disarticulated bones.

For the serial histology, the joint samples were prepared using first a hand-saw and then a low-speed wafering saw (Beuhler IsoMet 1000). The samples were fixed in 10% formalin for 3 days, and then decalcified in solutions of Cal-Ex (Fischer Scientific; 5.5%

Table 1 List of specimens used in this study. The last column specifies for which method each specimen was used.

Taxon	Specimen	Preservation	Method
Iguana iguana	UAMZ R951 (adult)	Frozen	Dissection, μCT, 3D rendering, serial histology
	ROM R 441 (subadult)	Skeletonized	Comparative osteology
Basiliscus basiliscus	ROM R 5539 (adult)	Skeletonized	Comparative osteology
	ROM R 5583 (subadult)	Skeletonized	Comparative osteology
Phrynosoma sp.	UAMZ R953 (subadult)	Frozen	μCT, 3D rendering
	TMP 1997.030.0321 (adult)	Skeletonized	Comparative osteology
	TMP 1997.030.0324 (adult)	Skeletonized	Comparative osteology
Pogona vitticeps	UAMZ R952 (adult)	Frozen	Dissection, μCT, 3D rendering, comparative osteology
	ROM 8514 (adult)	Skeletonized	Comparative osteology
Physignathus draconoides	TMP 1990.007.0347 (adult)	Skeletonized	Comparative osteology
Amblyrhynchus cristatus	AMNH R-29937 (adult)	Skeletonized	Comparative osteology
	AMNH R-114492 (adult)	Skeletonized	Comparative osteology
	AMNH R-114491 (young)	Skeletonized	Comparative osteology
Conolophus subcristatus	AMNH R-131308 (adult)	Skeletonized	Comparative osteology
	AMNH R-110168 (subadult)	Skeletonized	Comparative osteology
Conolophus pallidus	AMNH R-147848 (adult)	Skeletonized	Comparative osteology
Heloderma suspectum	TMP 1990.7.27 (young)	Skeletonized	Comparative osteology
	TMP 90.7.357 (subadult)	Skeletonized	Comparative osteology
Varanus albigularis	UAMZ R947 (adult)	Skeletonized	Comparative osteology
Varanus timorensis	UAMZ R901 (hatchling)	Skeletonized	Comparative osteology
Macrocephalosaurus chulsanensis	ZPAL Mg R I-21 (adult)	Fossil	Comparative osteology
	ZPAL Mg R I-23 (adult)	Fossil	Comparative osteology
Saichangurvel davidsoni	IGM 3-858 (adult)	Fossil	Comparative osteology
Primitivus manduriensis	MPUR NS 161 (subadult)	Fossil	Comparative osteology

Institutional abbreviations: AMNH, American Museum of Natural History; IGM, Institute of Geology, Mongolian Academy of Sciences, Ulaanbaatar, Mongolia; MPUR, Museo Paleontologico dell'Università di Roma, Rome, Lazio, Italy; New York, New York, USA; ROM, Royal Ontario Museum, Toronto, Ontario, Canada; TMP, Royal Tyrrell Museum of Palaeontology, Drumheller, Alberta, Canada; UAMZ, University of Alberta Museum of Zoology, Edmonton, Alberta, Canada; ZPAL, Institute of Palaeobiology, Polish Academy of Sciences, Warsaw, Poland.

hydrochloric acid and 0.12% EDTA, pH 2.0) for 17–28 days (according to the size of the sample). To speed up the decalcification process, the solution was replaced every 24 h and the samples were placed on a mechanical shaker for 8 h every day. Samples were rinsed in running tap water after the decalcification was completed, stored back in fixative for several hours, and then placed overnight in a tissue processor for clearing and paraffin infiltration. Finally, the samples were embedded in blocks of paraffin wax and placed on ice for about an hour before starting sectioning. The serial sections were cut at 5 μm using a rotary microtome (Leica 2025) and mounted on charged glass slides (Fisherbrand, Superfrost Plus). Sections for the right ISJ of the *I. iguana* sample were cut axially (i.e. transverse or cross-sections), anterior to posterior, and posterior to anterior, in order to capture the articulation of each sacral rib with the ilium separately. The left ISJ of the same *I. iguana* specimen was used to cut longitudinal or coronal sections (ventral to dorsal), in order to capture the two sacral ribs in articulation with the ilium at the same time. We then applied Masson's trichrome staining, following the protocol in Appendix S1.

The thin sections were imaged using a Nikon DS-FI3 camera mounted on a Nikon Eclipse E600 POL microscope, and Nikon NIS Elements (ver. 4.60) imaging software. Images of the thin sections were captured in plane and cross-polarized light.

Results

Osteology

The two sacral vertebrae in lizards bear ribs that tend to converge distally and form a contact between the posterior/posteroventral margin of the first sacral rib (sr-I) and the anterior/anterodorsal margin of the second sacral rib (sr-II). The extent of this contact never exceeds the distal half of the two ribs, and in general seems to vary from species to species. The two sacral ribs never fuse completely to the extent that the suture between them is obliterated in any of our study specimens (Table 1; Figs 1–3, 5, 7–12), as reported for some lizards by Hoffstetter & Gasc (1969). In fact, the μCT scans of *I. iguana*, *P. vitticeps* and *Phrynosoma* sp. show that both sacral ribs have separate, finished margins, and sometimes even a small gap between them (Figs 3, 7, 8).

The contact between sr-I and sr-II is more extensive in the extant *I. iguana*, *Conolophus pallidus*, *Amblyrhynchus cristatus*, and the fossil taxa *Macrocephalosaurus* and

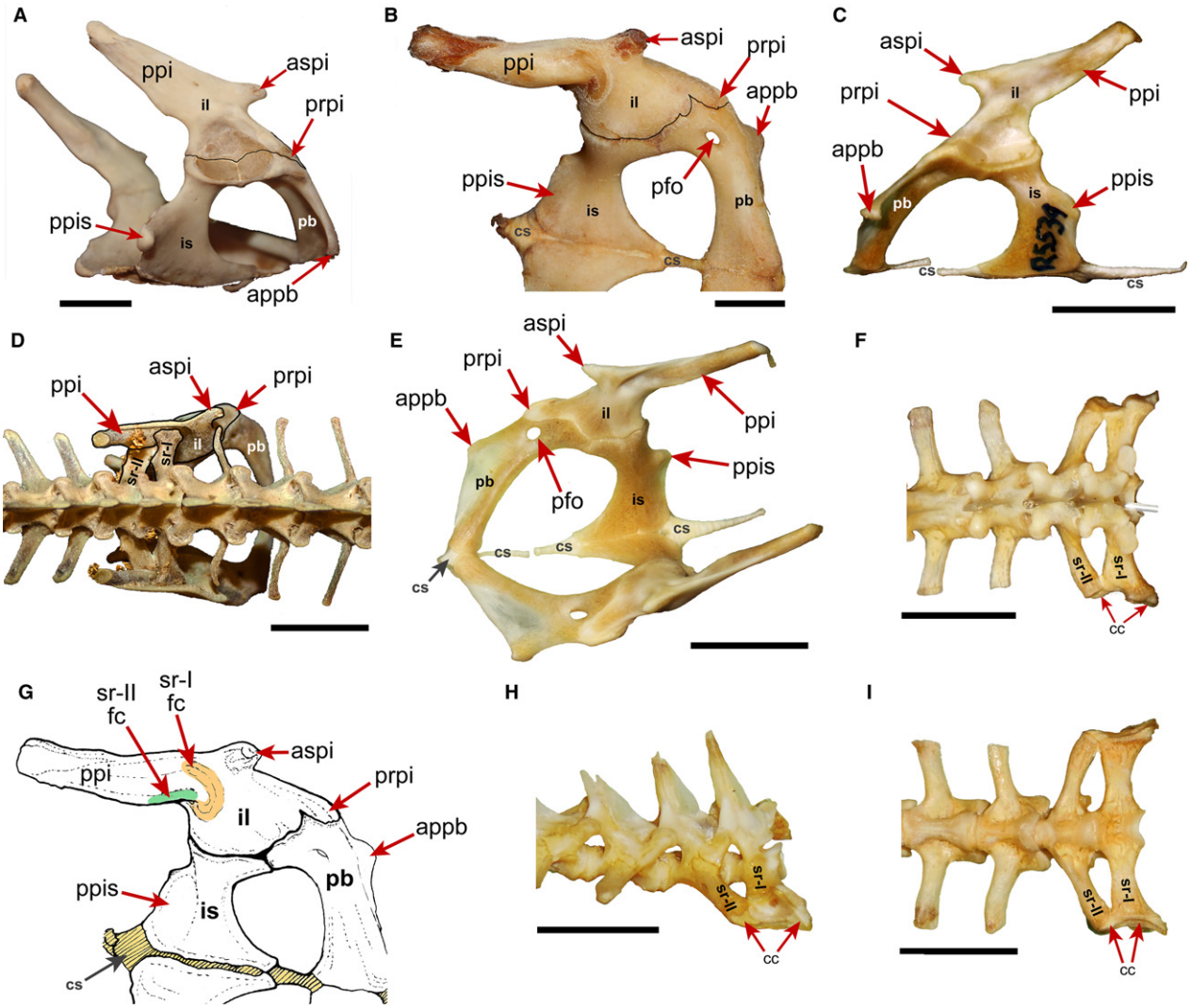

Fig. 1 Lizard iliosacral joint (ISJ) osteological terminology and examples: *Iguana iguana* [ROM R 441 (A, D)], *Varanus albigularis* [UAMZ R947 (B, G)] and *Basiliscus basiliscus* [ROM R 5539 (C, E, F, H, I)]. (A) Right pelvic girdle of *I. iguana* in lateral view showing the three pelvic bones (ilium, pubis and ischium) and relative processes. (B) Left pelvic girdle of *V. albigularis* in medial view showing the three pelvic bones (ilium, pubis and ischium) and relative processes. (C) Left pelvic girdle of *B. basiliscus* in lateral view showing the three pelvic bones (ilium, pubis and ischium) and relative processes. (D) Dorsal view of the sacral region and ISJs of *I. iguana*. (E) Right pelvic girdle of *B. basiliscus* in medial view showing the three pelvic bones (ilium, pubis and ischium) and relative processes. (F) Dorsal view of the sacral region and ISJs of *B. basiliscus*. (G) Diagram of the left pelvic girdle of *V. albigularis* in medial view showing the facets for the articulation of the two sacral ribs on the posterior process of the ilium. (H) Lateral view of the right sacral ribs of *B. basiliscus* showing the joint surface of articulation that they form to contact the posterior process of the ilium. (I) Ventral view of the sacral region and ISJs of *B. basiliscus*. Scale bars: 1 cm. appb, anterior process of the pubis; aspi, anterior supracetabular process of the ilium; car, cartilage; cs, symphyseal cartilage; fc, facet; fe, femur; il, ilium; is, ischium; pb, pubis; pfo, pubic foramen; ppi, posterior process of the ilium; ppis, posterior process of the ischium; prpi, preacetabular process of the ilium; sr-I, first sacral rib; sr-II, second sacral rib.

Saichangurvel (Figs 1–3, 5, 10, 11). In *Phrynosoma* sp. and *P. vitticeps*, sr-I overlaps the anterodorsal margin of sr-II, but in terms of length, the contact is limited to the very distal ends of the two ribs (Figs 7, 8). The contact is limited to the most distal tip of the two ribs also in *Basiliscus basiliscus*, *Heloderma suspectum*, *Physignatus draconoides*, and *Varanus albigularis* (Figs 1, 9, 12).

In general, sr-I is larger than sr-II in terms of distal expansion and/or dorsoventral thickness, or at most they are similar in size (e.g. *Macrocephalosaurus* and *Saichangurvel*: Fig. 2). The difference is quite emphasized in some taxa, such as *B. basiliscus*, and *P. draconoides*. In lateral view, sr-I is characterized by a C-shaped termination that forms most of the articulation with the ilium, and sr-II posteriorly (Figs 1, 9, 10, 12). As a consequence of the greater dorsoventral thickness of sr-I, and its C-shaped distal end, the contribution to the ISJ by sr-II is mostly ventral or posteroventral; dorsally, the first sacral rib forms the entire contribution to the ISJ.

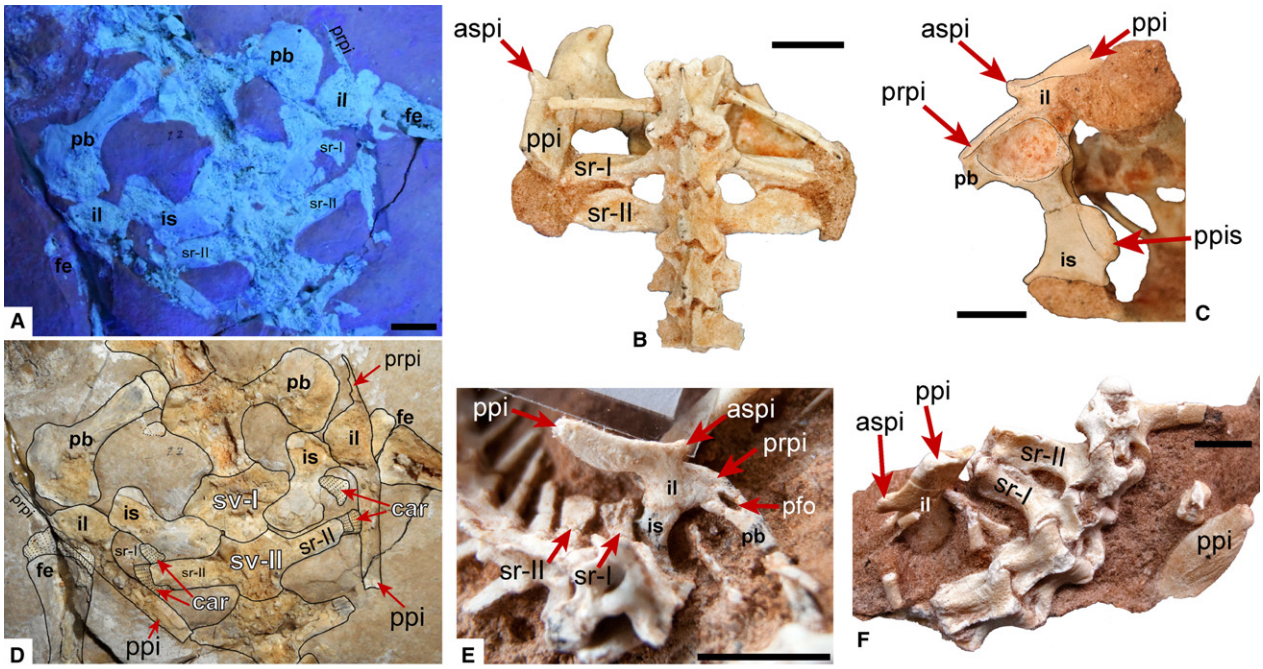

Fig. 2 Osteology of the iliosacral joint (ISJ) in some fossil lizards: *Primitivus manduriensis* [MPUR NS 161 (A, D)], *Macrocephalosaurus chulsanensis* [ZPAL Mg R I-23 (B, C) and ZPAL Mg R I-21 (F)], *Saichangurvel davidsoni* [IGM 3-858 (E)]. (A) Sacral region and ISJs of *P. manduriensis* in dorsal view, exposed to ultraviolet light and showing the preservation of cartilage at the distal ends of the sacral ribs. (B) Sacral region and left ISJ of *M. chulsanensis* in dorsal view. (C) Pelvic girdle of *M. chulsanensis* in lateral view. (D) Sacral region and ISJs of *P. manduriensis* in dorsal view photographed at natural light. (E) Left pelvic girdle in medial view and sacral region of *S. davidsoni*. (F) Disarticulated pelvic girdles and sacral region of *M. chulsanensis* in dorsal view. Scale bars: 1 cm. aspi, anterior supracetabular process of the ilium; car, cartilage; fe, femur; il, ilium; is, ischium; pb, pubis; pfo, pubic foramen; ppi, posterior process of the ilium; prpi, preacetabular process of the ilium; sr-I, first sacral rib; sr-II, second sacral rib; sv-I, first sacral vertebra; sv-II, second sacral vertebra.

The ilium in lizards is characterized by the presence of three main processes: (i) the posterior process – often referred to as the posterior iliac blade or post-iliac blade (Snyder, 1954; Borsuk-Białynicka, 2008; Gans et al. 2008) – projecting posterodorsally from the iliac shaft, and bearing the facets for articulation of the sacrals; (ii) the preacetabular process, located anteriorly to the acetabulum and overlapping the pubic head; and (iii) the supracetabular process – often referred to as the iliac tubercle or spine – located above the acetabulum, and anterodorsally oriented relative to the iliac shaft (Figs 1, 2, 7–11). All three iliac processes vary in shape and extent, and a correlation with the posture and locomotion abilities has been found at least for the supracetabular process (Snyder, 1954).

The posterior process is the only one of the iliac processes directly involved in the ISJ, being the part that articulates with the sacral ribs. In the specimens we examined, the main differences in the posterior iliac process regard its orientation in relation to the vertebral column (and to the ischium and pubis) and its shape and thickness in cross-section. Borsuk-Białynicka (2008) described how this process is almost perpendicular to the vertebral column in the non-squamate lepidosaur *Sphenodon*, and is greatly tilted posteriorly in lizards. We found that in the marine iguana, *A. cristatus*, the posterior iliac process is almost horizontal and parallel to the vertebral column (Fig. 10). A similar condition occurs in the water monitor *V. albigularis*, and *H. suspectum*, though to a lesser degree, with the posterior iliac process slightly more posterodorsally oriented in relation to the vertebral column (Figs 1B, 9). The process clearly forms a much greater angle with the column in *P. vitticeps*, *I. iguana*, *B. basiliscus*, *Phrynosoma*, and the fossil taxa, *Macrocephalosaurus* and *Saichangurvel* (Figs 1, 2, 7, 8). The main portion of the posterior iliac process is fairly cylindrical in *V. albigularis* and *H. suspectum* (although quite narrow and elongated only in the latter; Figs 1, 9, 12), while it is more elliptical in most iguanian specimens (*Amblyrhynchus*, *P. vitticeps*, *I. iguana* and *Saichangurvel*: Figs 1–3, 7, 8, 10, 11). The process is quite laterally flattened in *B. basiliscus*, *Phrynosoma* and *Macrocephalosaurus*, even taking into account that taphonomic processes may have emphasized the condition in the fossil specimen ZPAL Mg R I-23 (Figs 1, 2, 7).

For the preacetabular and supracetabular iliac process, the terminology in the literature is inconsistent: what we call here the preacetabular process can be hard to discern when there is complete fusion of the three pelvic bones, and authors tend to not address this process and often use ‘preacetabular’ for the iliac tubercle (i.e. the supracetabular process; Snyder, 1954, 1962; Borsuk-

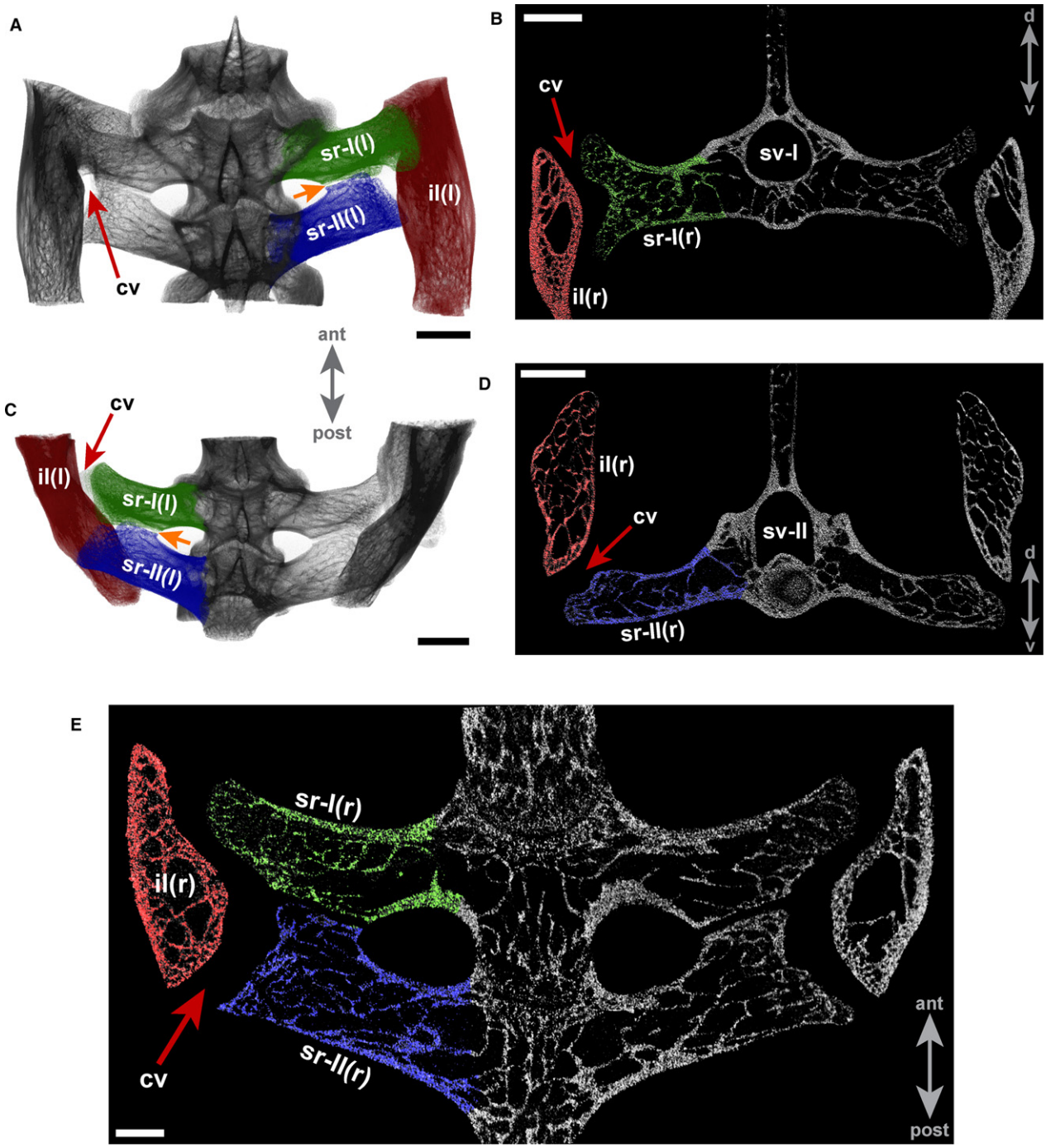

Fig. 3 Micro-computed tomography (μCT) of the iliosacral joint (ISJ) of *Iguana iguana* (UAMZ R951). (A) Three-dimensional reconstruction of the ISJ from the μCT scans showing a dorsal view of the structure. (B) Frame of the ISJ from the μCT scans showing the ilium and first sacral rib in cross-section. (C) Three-dimensional reconstruction of the ISJ from the μCT scans showing the structure in ventral view. (D) Frame of the ISJ from the μCT scans showing the ilium and second sacral rib in cross-section. (E) Frame of the ISJ from the μCT scans showing an overview of the articulation in longitudinal section. The orange arrows in (A) and (C) point at the gap between the two sacral ribs that the histological sections revealed to be a syndesmotic suture (Fig. 4C,D). Scale bars: 1 cm. ant, anterior; cv, cavity; il, ilium; l, left; post, posterior; r, right; sr-I, first sacral rib; sr-II, second sacral rib.

Białynicka, 2008). We prefer to use an anatomical terminology that best reflects the topology of these processes, taking into account their relative position to one another and to the iliac shaft. The preacetabular process is particularly long in *B. basiliscus* (especially visible in the disarticulated specimen ROM R 5583: Fig. 1C, E), and

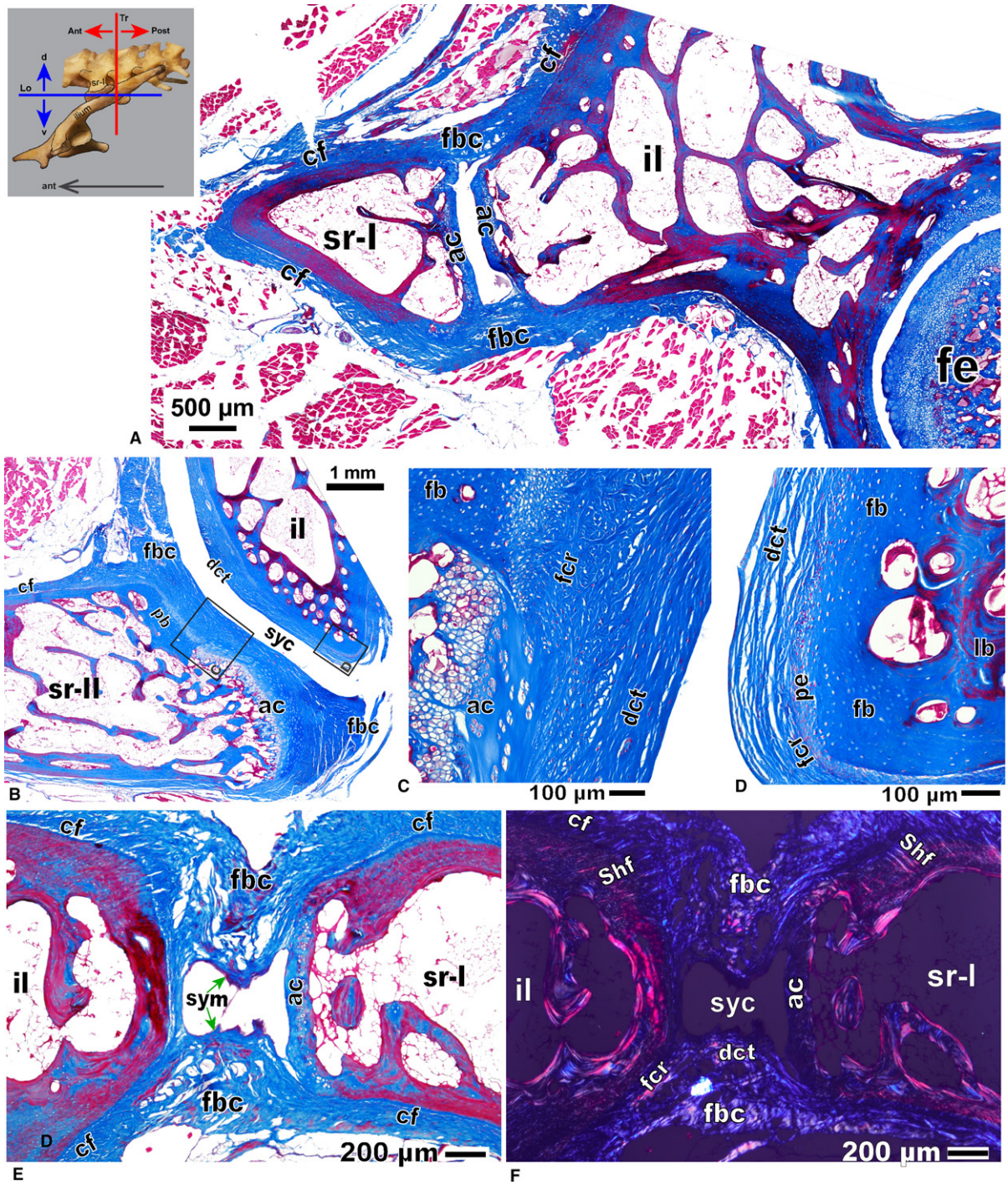

Fig. 4 Histology of the iliosacral joint (ISJ) of *Iguana iguana* (UAMZ R951). (A) Transverse section of the ISJ, showing an overview of the contact between the first sacral rib and the ilium, with also the hip joint (between the acetabulum and femur) visible on the right. (B) Overview of the contact between sacral ribs and the ilium in transverse section (close to the transition to sr-II). (C) Close-up of the articular surface of sr-II. (D) Close-up of the articular surface of the ilium. (E) Close-up of the contact between the first sacral rib and the ilium at plane-polarized light. (F) Close-up of the contact between the first sacral rib and the ilium at cross-polarized light. The thin sections pictured in (B), (C), (E) and (F) are cut close to the transition from sr-I to sr-II. In (E) and (F), the ISJ cavity reaches its narrowest point recorded throughout the transverse section series. ac, articular cartilage; ant, anterior; cf, collagen fibres; d, dorsal; dct, dense connective tissue; fb, fibrous bone; fbc, fibrous capsule; fcr, fibrocartilage; fe, femur; il, ilium; lb, lamellar bone; Lo, longitudinal plane of sectioning; pe, periosteum; post, posterior; r, right; Shf, Sharpey's fibres; sr-I, first sacral rib; sr-II, second sacral rib; syc, synovial cavity; sym, synovial membrane; Tr, transversal plane of sectioning; v, ventral.

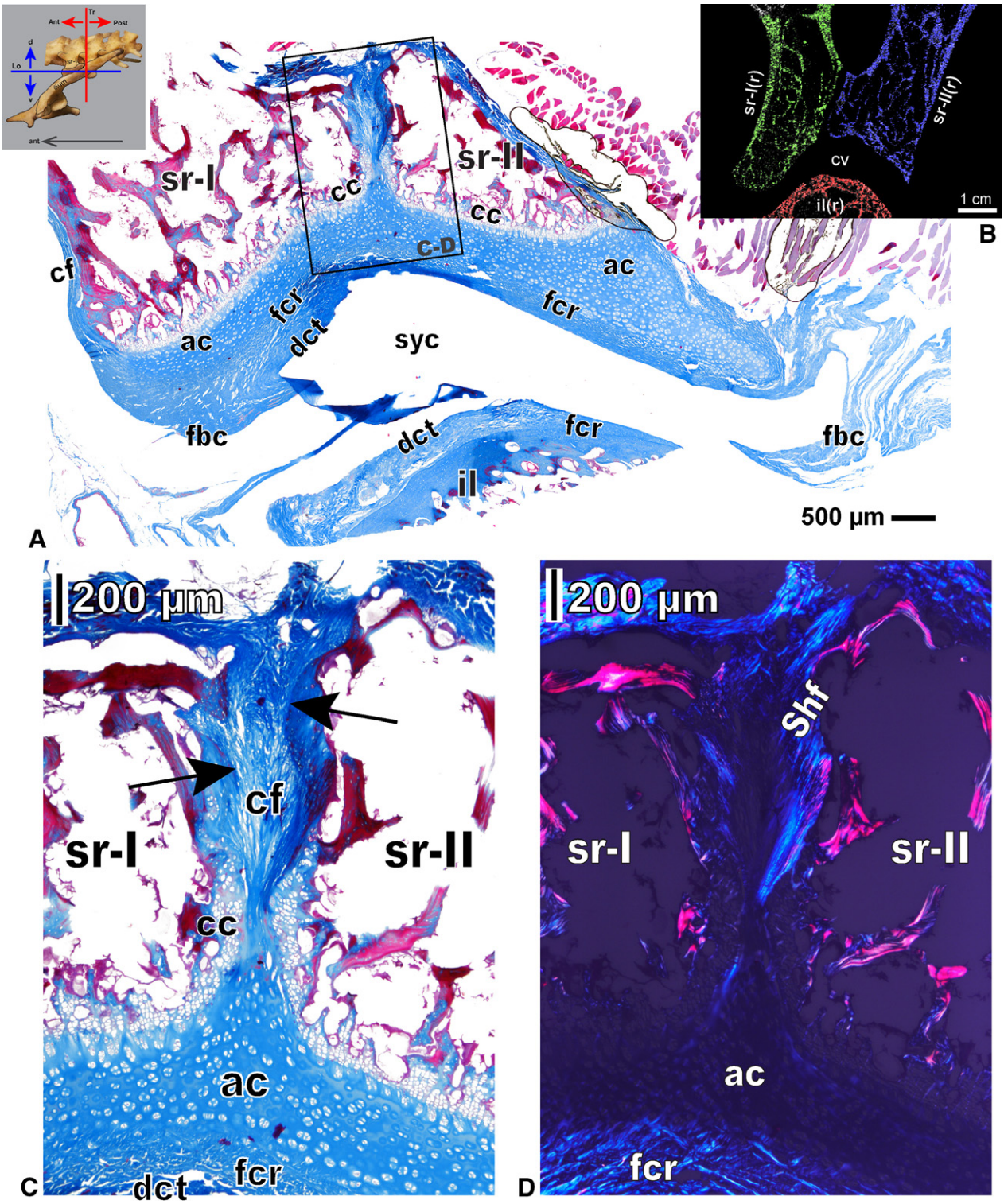

Fig. 5 Histology of the iliosacral joint (ISJ) of *Iguana iguana* (UAMZ R951). (A) Longitudinal section of the ISJ, showing the contact between the two ribs and the ilium close to the ventral edge of the structure. (B) Frame of the right ISJ from the micro-computed tomography (µCT) scans showing the gap between the sacral ribs and the ilium for comparison with the histological section in (A). (C) Longitudinal section of the suture between sr-I and sr-II at plane-polarized light. (D) Longitudinal section of the suture between sr-I and sr-II at cross-polarized light. The black arrows in (C) point at the edge between the bone and collagen fibres at the suture between the two sacral ribs, while closer to the articular cartilage cap these fibres are contacting a layer of calcified cartilage. ac, articular cartilage; ant, anterior; cc, calcified cartilage; cf, collagen fibres; cv, cavity; d, dorsal; dct, dense connective tissue; fbc, fibrous capsule; fcr, fibrocartilage; fe, femur; il, ilium; Lo, longitudinal plane of sectioning; post, posterior; r, right; Shf, Sharpey's fibres; sr-I, first sacral rib; sr-II, second sacral rib; syc, synovial cavity; Tr, transversal plane of sectioning; v, ventral.

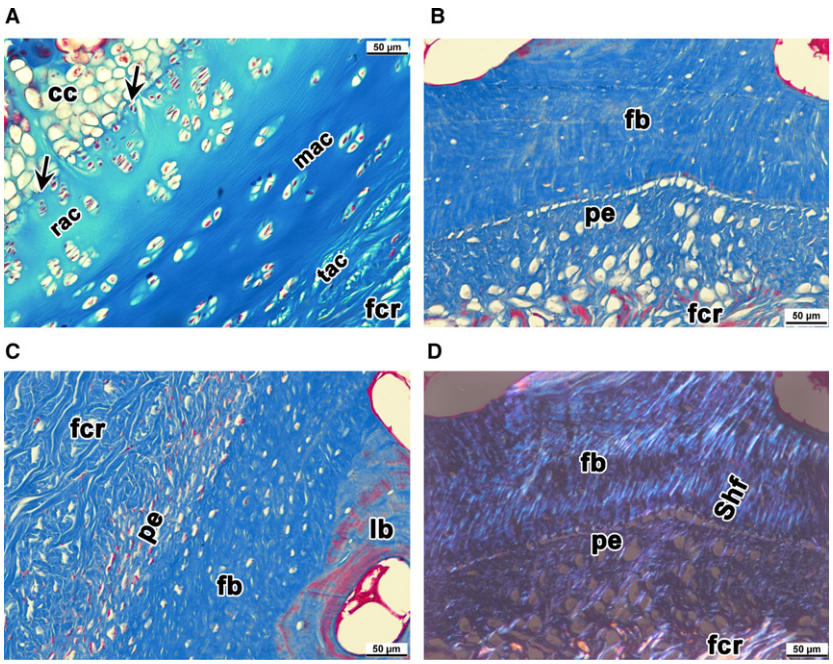

Fig. 6 Detail of the tissues of the iliosacral joint (ISJ) elements of *Iguana iguana* (UAMZ R951) from the transverse section series. (A) Close-up of the distal edge of the first sacral rib at plane-polarized light. (B) Close-up of the tissues along the medial margin of the ilium, away from the contact with the sacral ribs (at plane-polarized light). (C) Close-up of the ilium in correspondence of the articular facet for the first sacral rib. (D) Same thin section captured in (B) but with cross-polarized light. Secondary osteons (lamellar bone) are found more internally on the ilium, at the transition towards the trabecular region of the bone (C). Instead, closer to the periosteal region of the ilium the bone shows abundance of Sharpey's fibres and small lacunae (fibrous bone). Fibrocartilage is overlying the periosteum on the ilium (B–D), while surrounding the articular cartilage in the sacral ribs (A). The different zones of the articular cartilage on the sacral ribs are visible in (A), including the tidemark (black arrows) between the calcified cartilage and radial zone. cc, calcified cartilage; fb, fibrous bone; fcr, fibrocartilage; lb, lamellar bone; mac, middle (or transitional) zone of the articular cartilage; pe, periosteum; rac, radial (or deep) zone of the articular cartilage; Shf, Sharpey's fibres; tac, tangential (or superficial) zone of the articular cartilage.

exceptionally long in the dolichosaur *Primitivus manduriensis* (Fig. 2A, D). The degree of development of this process is fairly similar amongst the rest of the specimens here examined.

The supracetabular process changes in the length, width and shape of its distal end. Specimens of *Basiliscus* and *Pogona* have relatively longer and more slender processes that taper distally to pointed tips (Figs 1, 8). In *Varanus albigularis*, the supracetabular process is overall wider and remains cylindrical throughout (Figs 1B, 12A). In *I. iguana*, *Saichangurvel*, *Phrynosoma* and *Macrocephalosaurus* this process is relatively broad proximally, quite elliptical in cross-section, and only weakly tapers distally, ending in a fairly rounded tip (Figs 1, 2, 7). A short process, quite broad across the dorsoventral axis, and fairly blunt distally characterizes *Amblyrhynchus* (Fig. 10), while in *Heloderma* it is basically absent, with barely a tiny spur remaining (Fig. 9).

Histology

Results from the serial histology are illustrated in Figs 4–6. The presence of a large gap between the ilium and sacral ribs is apparent in the µCT scans of the *I. iguana*, *Phrynosoma* sp. and *P. vitticeps* specimens (Figs 3, 5, 7, 8). From the serial histology of the *I. iguana* sample, we found that this space is partially occupied by articular cartilage, fibrocartilage and dense connective tissue, which are variably present at the edges of the bones (Figs 4–6). However, a gap in our thin sections is present between the distal ends of the sacral ribs and the medial surface of the ilium throughout both transverse and longitudinal series, and it is continuous even when transitioning from sr-I to sr-II (Fig. 4). The gap becomes narrower close to the transition from sr-I to sr-II, as visible in Fig. 4E-F.

Articular cartilage is found at the distal ends of the sacral ribs, connected to the subchondral bone via a conspicuous layer of calcified cartilage (Figs 4–6A). The transitional zone of the articular cartilage is particularly thick in comparison to both the radial and tangential zones (Fig. 6A). Both transverse and longitudinal series of thin sections of the *I. iguana* ISJ show that the large cap of articular cartilage is continuous between the two ribs, which join to form a single structure for articulation with the posterior process of the ilium. Fibrocartilage surrounds the articular cartilage on both sacral ribs virtually in all our thin sections (Figs 4B-C, E-

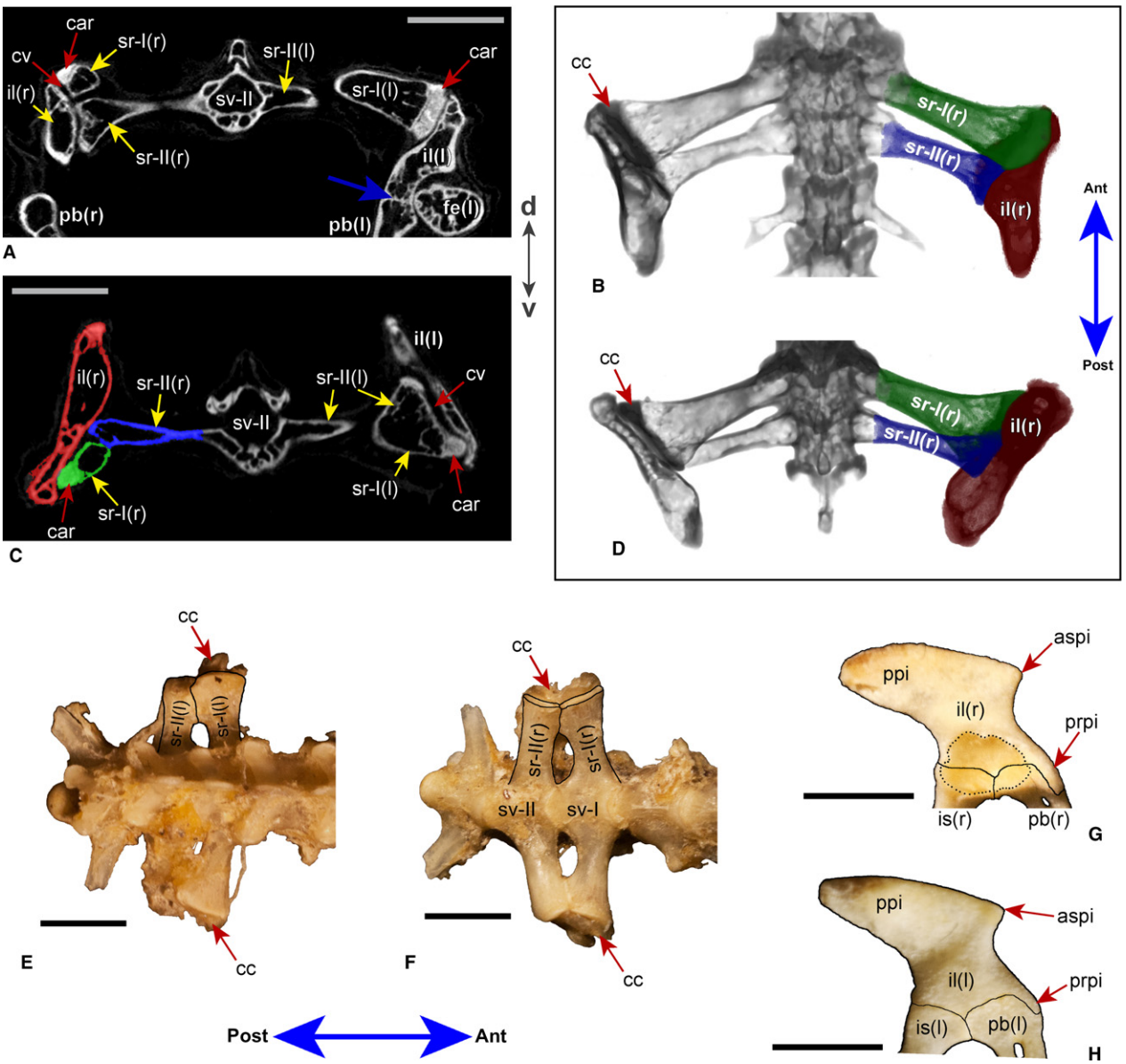

Fig. 7 Osteology and micro-computed tomography (μCT) of the iliosacral joint (ISJ) of *Phrynosoma*: UAMZ R953 (A–D), TMP 1997.030.0324 (E,F) and TMP 1997.030.0321 (G,H). (A) Cross-section of the sacral region and ISJs from the μCT scans of UAMZ R953. (B) Three-dimensional reconstruction of the sacrum and ISJs from the μCT scans of UAMZ R953 in dorsal view. (C) Cross-section of the sacral region and ISJs from the μCT scans of UAMZ R953 close to the contact between sr-I and sr-II. (D) Three-dimensional reconstruction of the sacrum and ISJs from the μCT scans of UAMZ R953 in ventral view. (E) Sacral region of the vertebral column of specimen TMP 1997.030.0324 in dorsal view. (F) Sacral region of the vertebral column of specimen TMP 1997.030.0324 in ventral view. (G) Right ilium of specimen TMP 1997.030.0321 in lateral view. (H) Left ilium of specimen TMP 1997.030.0321 in medial view. The blue arrow in (A) indicates the position of the suture between the ilium and the pubis. Scale bars: 1 cm. ant, anterior; aspi, anterior supracetabular process of the ilium; car, cartilage; cc, calcified cartilage; cs, symphyseal cartilage; cv, cavity; d, dorsal; fe, femur; il, ilium; is, ischium; l, left; pb, pubis; post, posterior; ppi, posterior process of the ilium; prpi, preacetabular process of the ilium; r, right; sr-I, first sacral rib; sr-II, second sacral rib; sv-I, first sacral vertebra; sv-II, second sacral vertebra; v, ventral.

F; 5; 6A). The distinction between articular (hyaline) cartilage and fibrocartilage is particularly evident under cross-polarized light, which emphasizes the typical arrangement of the cross-laid collagen fibres of the latter (Fig. 5D).

In comparison to the sacral ribs, the ilium has a smaller amount of articular cartilage, which is not found throughout the extent of the ISJ in the serial sections. This is not completely unexpected, as the portion of the posterior process of the ilium that contacts the sacrals seems to be limited to the outline of the articular facets for sr-I and sr-II. This outline is often visible macroscopically on the posterior process of the ilium (medial surface), marked usually by the presence of

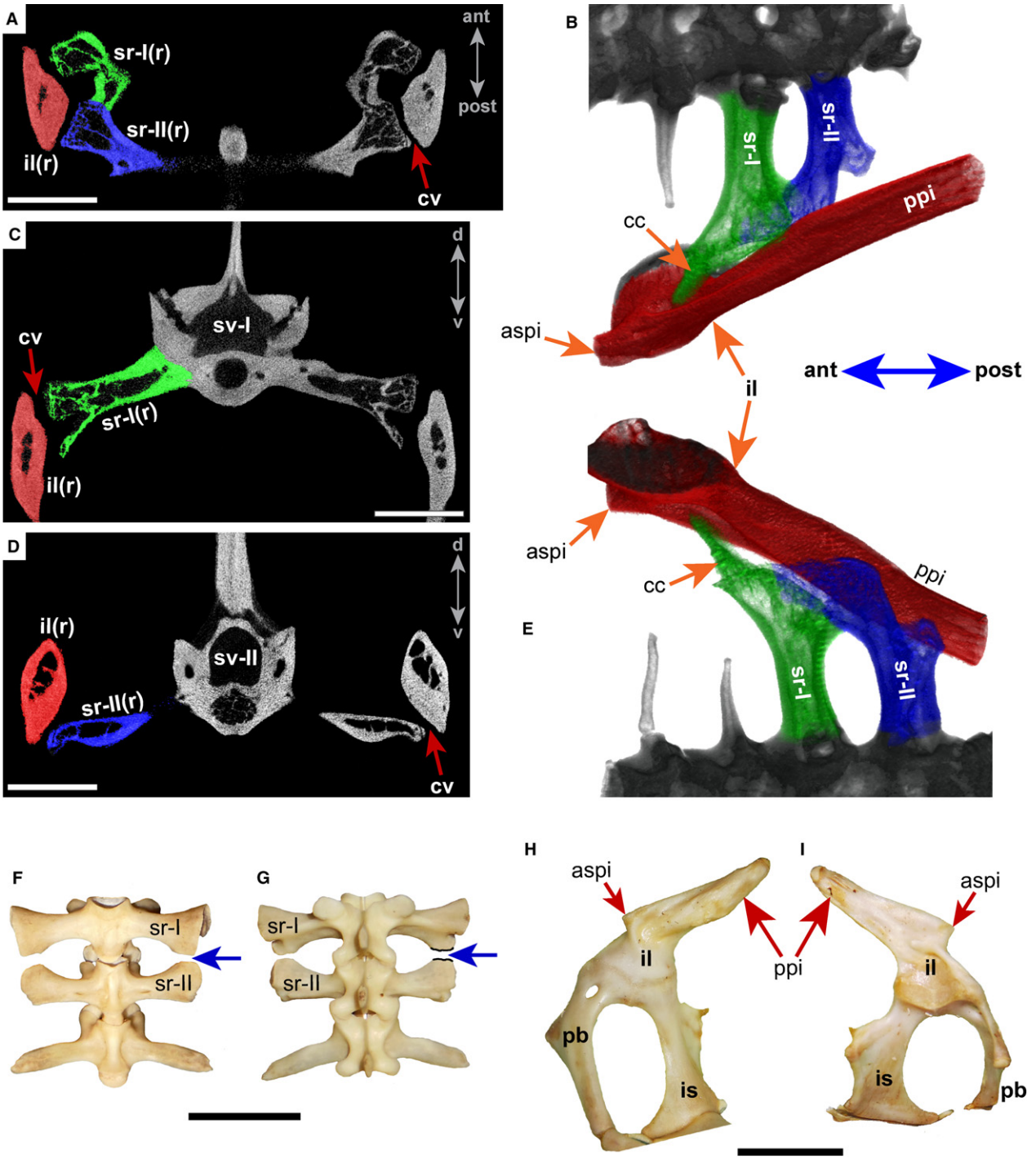

Fig. 8 Osteology and micro-computed tomography (μCT) of the iliosacral joint (ISJ) of *Pogona vitticeps*, specimens. UAMZ R952 (A–E) and ROM 8514 (F–I). (A) Longitudinal section of the sacral region and ISJs from the μCT scans of UAMZ R952. (B) Three-dimensional reconstruction of the left sacrum and ISJ from the μCT scans of UAMZ R952 in dorsal view. (C) Cross-section of the sacral region and ISJs from the μCT scans of UAMZ R952 at the contact between the first sacral rib and the ilium. (D) Cross-section of the sacral region and ISJs from the μCT scans of UAMZ R952 at the contact between the second sacral rib and the ilium. (E) Three-dimensional reconstruction of the left sacrum and ISJ from the μCT scans of UAMZ R952 in ventral view. (F) Sacral region of the vertebral column of ROM 8514 in ventral view. (G) Sacral region of the vertebral column of ROM 8514 in dorsal view. (H) Right ilium of ROM 8514 in medial view. (I) Right ilium of ROM 8514 in lateral view. The two sacral ribs in (F) and (G) are distally disarticulated and show the finished margin of both ribs at the level of their contact. Scale bars: 1 cm. ant, anterior; aspi, anterior supracetabular process of the ilium; cc, calcified cartilage; cs, cartilage symphysis; cv, cavity; d, dorsal; fe, femur; il, ilium; is, ischium; l, left; pb, pubis; post, posterior; ppi, posterior process of the ilium; r, right; sr-I, first sacral rib; sr-II, second sacral rib; sv-I, first sacral vertebra; sv-II, second sacral vertebra; v, ventral.

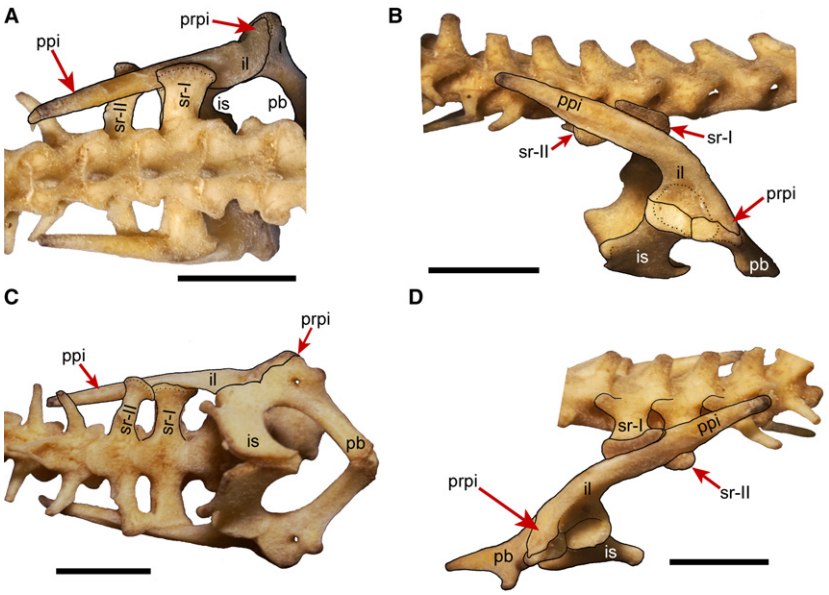

Fig. 9 Osteology of the iliosacral joint (ISJ) of *Heloderma suspectum* (TMP 90.7.357). (A) Sacral region and ISJs in dorsal view. (B) Sacral region and right pelvic girdle in lateral view. (C) Sacral region and ISJs in ventral view. (D) Sacral region and left pelvic girdle in lateral/anterolateral view. Noticeable is the absence of the supracetabular process of the ilium on its anterodorsal margin (cf. Fig. 1). Scale bars: 1 cm. il, ilium; is, ischium; pb, pubis; ppi, posterior process of the ilium; prpi, preacetabular process of the ilium; sr-I, first sacral rib; sr-II, second sacral rib.

cartilage and/or a convexity on the bone (Figs 1, 3, 8–12). Fibrocartilage is more frequent on the ilium, surrounding often the periosteum directly, and associated with the presence of dense connective tissue (externally) and Sharpey's fibres into the bone (fibrous bone; Figs 4E-F; 6B–D).

The collagen fibre bundles bordering the ilium and sacral ribs anchor into the bones and form Sharpey's fibres around the ISJ and along the contact between sr-I and sr-II (Figs 4E-F; 5C-D, 6B, D). The Sharpey's fibres are particularly dense in correspondence to the ligament connecting the ilium to the sacral ribs; they are all parallel to each other, and with the same orientation of the ligament fibres anchoring to the bone.

Finally, another smaller gap is visible in the μCT scans of the *I. iguana* sample at the contact of the two sacral ribs (Figs 3, 5B). In thin section, this space is filled with dense collagen fibres that are interrupted distally by the articular cartilage capping sr-I and sr-II (Fig. 5). The fibres seems to either attach directly to the cortical bone of the two sacral ribs (more proximally) or to a layer of calcified cartilage present on both sides of this contact (more distally; Fig. 5C, D).

Discussion

The ISJ in lizards is a synovial joint

Micro-CT imaging of the iguanian ISJ region revealed large gaps between the sacral ribs and the ilium, but the type of joint can only be determined using histological techniques. There are two major categories of joints: (i) diarthroses (synovial joints), which are the type of joints that allow for greater mobility; and (ii) synarthroses, which provide no or limited mobility (Barnett et al. 1961; Kardong, 2006). Synovial joints are characterized by four main histological features: (i) a cavity filled with synovial fluid; (ii) a membrane encasing the cavity and secreting the fluid; (iii) articular cartilage at the edges of the contacting bones; and (iv) a multilayered dense fibrous tissue surrounding the membrane and forming the capsule bordering the entire structure (Barnett et al. 1961; Martin et al. 1998b; Archer et al. 2003; Kardong, 2006). Articular cartilage is a special type of hyaline cartilage that lacks a perichondrium and is characterized by a specific internal zonation of collagen fibres and chondrocytes (Lambert, 1944; Martin et al. 1998a; Hall, 2005). Articular cartilage persists in skeletally mature individuals, even after hyaline cartilage has been fully replaced by bone during growth (Archer et al. 2003; Bilezikian et al. 1996).

Synarthroses lack a cavity and articular cartilage, and are subdivided into: (i) synostoses, where the contact is bone-to-bone; (ii) synchondroses, where the contact is lined by intervening cartilage; and (iii) syndesmoses, where fibrous connective tissue intervenes between the contacting elements (Barnett et al. 1961; Kardong, 2006). Among synarthroses, mobility is found in syndesmotic joints, where the fibrous connective tissue allows for some movement between the articulating elements. Cartilage is less rigid than bone and typically functions as a cushion between the articulating elements; however, its shock-absorbing properties are more limited compared for instance with fibrous connective tissue (Martin et al. 1998b; Hall, 2005; Bilezikian et al. 1996).

According to the results of our serial histology, the contact between the sacral ribs and the ilium is characterized by the presence of articular cartilage and/or fibrocartilage, and a cavity surrounded by dense fibrous connective tissue (Figs 4–6). These elements together clearly define the ISJ as a synovial joint. Although fibrocartilage is not always found

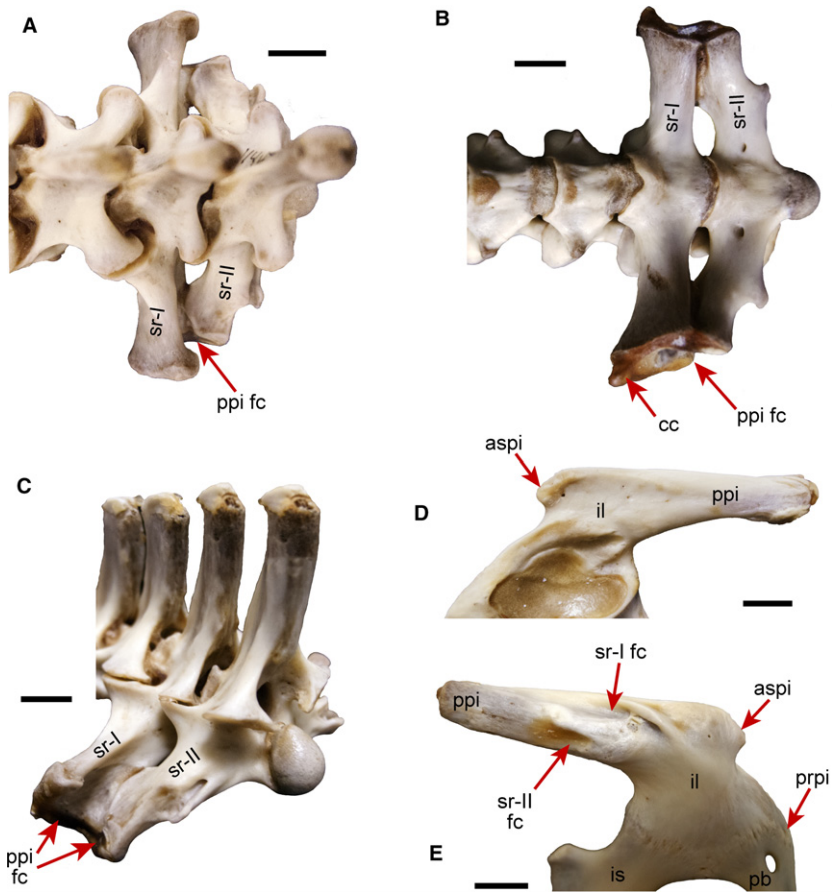

Fig. 10 Osteology of the iliosacral joint (ISJ) of *Amblyrhynchus cristatus* (AMNH R-114492). (A) Sacrals in dorsal view. (B) Sacrals in ventral view. (C) Left sacral ribs in posterolateral view showing the joint surface of articulation for the posterior process of the ilium. (D) Left ilium in lateral view. (E) Left ilium in medial view with emphasis on the position of the facets for the two sacral ribs on the posterior process. Scale bars: 1 cm. aspi, anterior supracetabular process of the ilium; car, cartilage; fc, facet; il, ilium; is, ischium; pb, pubis; ppi, posterior process of the ilium; prpi, preacetabular process of the ilium; sr-I, first sacral rib; sr-II, second sacral rib.

in synovial joints and it is not considered to be a defining feature for this type of joint, it has been observed in some human joints, such as the knee joint (Martin et al. 1998b), in the form of fibrocartilaginous discs (or menisci), as well as in the hip joint of several extant sauropsids (Tsai & Holliday, 2015). Our results are consistent with those of Tsai & Holliday (2015) for lepidosaurs, where thick layers of fibrocartilage cap or partially border the articular cartilage at the proximal epiphysis of the femur, similarly to crocodylians and in contrast to birds and turtles, for which much thinner layers or small patches of fibrocartilage are involved in the same joint.

Wolff (1990) defined the acetabulum (i.e. the junction of the three pelvic bones: ilium, ischium and pubis) as the joint cavity for the femoral head and, in a very similar mode, the distal ends of the two sacral ribs join together to form a joint cavity for articulation with the posterior process of the ilium. This comparison between the ISJ and the hip joint can be directly observed also in our thin sections (Fig. 4A) and μCT scans (Fig. 7A), where both articulations are visible. This arrangement is consistent with the fact that the distal cap of articular cartilage and the cavity between the sacral ribs and the ilium are continuous from sr-I to sr-II in the *I. iguana* sample (Fig. 5A). Moreover, the suture between sr-I and sr-II being interrupted by this articular cartilage further demonstrates that the two sacral ribs converge to form a single contacting surface for the ilium (Fig. 5). The position of the articular surface for the sacral ribs along the posterior process of the ilium varies interspecifically (see also below), and in our thin sections articular cartilage is found on the ilium only in a limited area of the contact with the distal margins of the sacral ribs (Fig. 4A). More frequently, in the serial histology of the *I. iguana* sample, we found fibrocartilage or simply dense connective tissue separating the bone of the ilium from the joint cavity formed by sr-I and sr-II (Figs 4; 5A; 6B-D).

Among all the specimens we analysed, a joint cavity formed by the two sacral ribs for articulation with the ilium is always present and macroscopically visible in skeletonized specimens (Figs 1D, F, H-I; 2B, E-F; 7E-F; 8F-G; 9C; 10A-C;

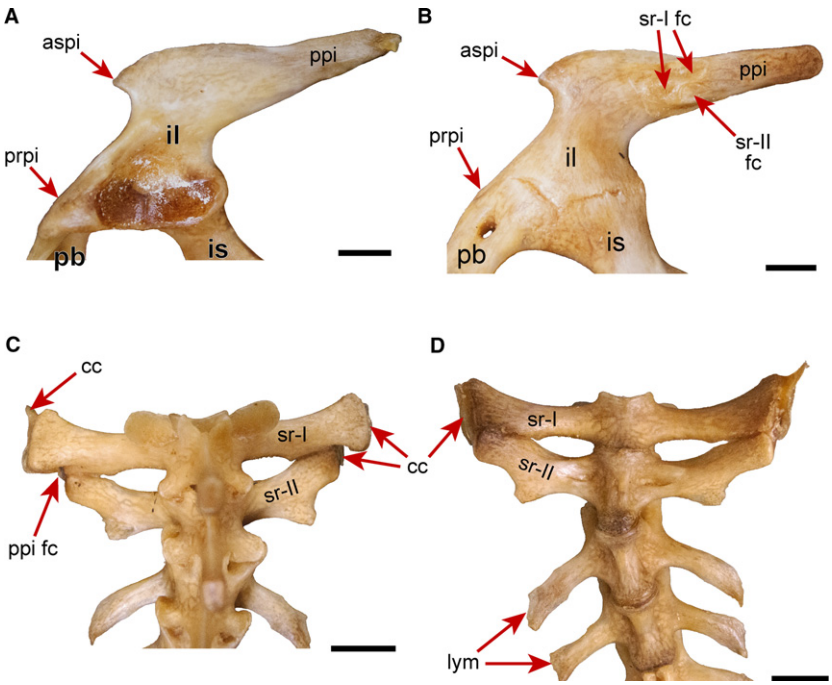

Fig. 11 Osteology of the iliosacral joint (ISJ) of *Conolophus pallidus* (AMNH R-147848). (A) Left pelvic girdle in lateral view. (B) Right pelvic girdle in medial view, showing the position of the facet for the two sacral ribs on the posterior process. (C) Sacral and post-sacral vertebrae in dorsal view. (D) Sacral and post-sacral vertebrae in ventral view. In (C) and (D), two vertebrae bearing distally grooved ribs (or lymphapophyses) are present posterior to the second sacral vertebra. Scale bars: 1 cm. aspi, anterior supracetabular process of the ilium; car, cartilage; fc, facet; il, ilium; is, ischium; lym, lymphapophysis; pb, pubis; ppi, posterior process of the ilium; prpi, preacetabular process of the ilium; sr-I, first sacral rib; sr-II, second sacral rib.

11C-D; 12), suggesting that potential variation in the different limbed lizards is not in the type of joint, but in the features of the bones involved and possibly the associated musculature. A certain variability is observed for the shape of the two articular surfaces across the analysed taxa (Table 1). We established that the two sacral ribs join together distally to form an articular cavity (for the contact with the ilium), and its concave shape is easily observed in the ct-scans (Figs 3; 5B, 7A–D; 8A–B, E) or in lateral views (Figs 1H; 10C; 12B, D) of some of the specimens. However, for the ilium, the shape of the articular facet for the joint cavity formed by the two sacral ribs is not always round. For instance, the medial surface of the posterior iliac process is fairly flat in *Basiliscus*, *Phrynosoma*, *Macrocephalosaurus* and *Conolophus* (Figs 1E; 2B; 7H; 11B). This variation in shape of the articular surface of the ilium most likely affects the mobility of the ISJ.

Interestingly, a study on paralysed chicken embryos conducted by Drachman & Sokoloff (1966) demonstrated how the lack of muscle contractions during the development of the embryo can prevent the formation of typically synovial joints (e.g. knee and ankle joints), affecting the morphogenesis of the articular surfaces. In their experiments, paralysed embryos either completely failed to develop a cavity between the contacting bones or only a partial cavity developed, with the joint space being filled by fibrous or cartilaginous connective tissue. The articular surfaces of the contacting bones were also flat and distorted rather than forming a ball-and-socket joint typical of the articulations under analysis (Drachman & Sokoloff, 1966). This study reveals that: (i) synovial cavities cannot form if there is lack of skeletal muscle contractions during embryonic development; and (ii) lack of muscle contractions (i.e. lack of movement) alters the surface morphology of the developing articular surfaces. By comparison, we can infer that the ISJ in limbed lizards, as a synovial joint, must have some mobility, and more so in those taxa where the concavity formed by the two sacral ribs is in contact with a fairly rounded posterior process of the ilium (e.g. *I. iguana*, *V. albigularis*, *P. vitticeps*).

Despite the rounded shape of the facet for articulation of the sacral ribs on the medial surface of the posterior iliac process, the rest of this process is elongated and sandwiched between the dorsal and ventral margins of the cavity formed by the two sacral ribs. This configuration would prevent a translation or a complete rotation of the ilium, as it does happen for instance for the femur within the acetabulum (Snyder, 1954; Oldham & Smith, 1975; Irschick & Jayne, 1999). However, during the dissections of *I. iguana* UAMZ R951 and *P. vitticeps* UAMZ R952, we noticed that the ilium can be twisted while still in articulation with the sacral ribs. A limited torsion (or axial rotation) of a few degrees about parallel to the vertebral column, for instance when lizards abduct the hip during locomotion, would certainly be possible. The presence of fibrocartilage within the lizard ISJ suggests that while the hindlimb is being protracted or retracted, the ISJ may also serve a shock-absorbing function, similar to what occurs with the joint discs in the knee or ankle articulations (Carey, 1922; Drachman & Sokoloff, 1966; Martin et al. 1998b; Irschick & Jayne, 1999).

The shape of the articular surface on the posterior process of the ilium is more complex in taxa such as *Amblyrhynchus* and *Heloderma*, where the contacting surface with the joint

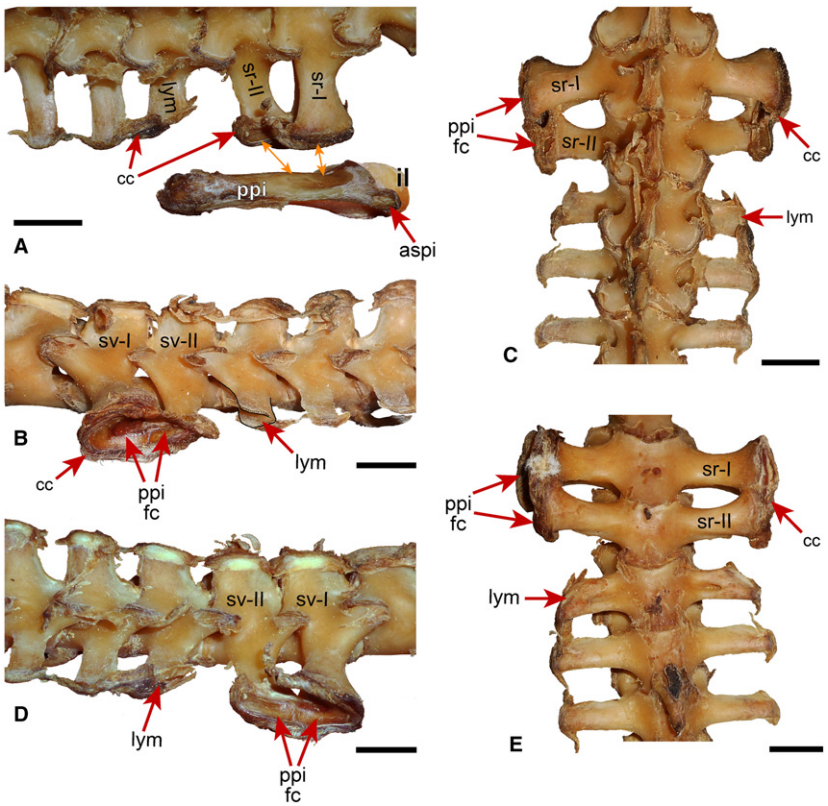

Fig. 12 Osteology of the iliosacral joint (ISJ) of *Varanus albigularis* (UAMZ R947). (A) Right sacrum, post-sacral vertebrae and ilium in dorsal view showing the presence of abundant cartilage at the distal ends of the sacral ribs and single lymphapophysis as well as on the ilium. (B) Sacrals and post-sacrals in left lateral view showing the joint articular facet formed by the two sacral ribs for the contact with the posterior process of the ilium, and the distally grooved lymphapophysis. (C) Sacral and post-sacral region of the vertebral column in dorsal view. (D) Sacrals and post-sacrals in right lateral view. (E) Sacral and post-sacral region of the vertebral column in ventral view. The orange arrows in (A) indicate the position of the articulation between the sacral ribs and the posterior process of the ilium. Scale bars: 1 cm. aspi, anterior supracetabular process of the ilium; cc, calcified cartilage; fc, facet; il, ilium; lym, lymphapophysis; ppi, posterior process of the ilium; prpi, preacetabular process of the ilium; sr-I, first sacral rib; sr-II, second sacral rib; sv-I, first sacral vertebra; sv-II, second sacral vertebra.

formed by the sacral ribs is crested (Figs 9A; 10E). Further observations would be necessary to assess how this shape can affect the movement at the ISJ, but it is reasonable to assume that a crested surface would be less favourable to either rotation or translation in comparison to any smooth, rounded surface. In taxa where the posterior process of the ilium is flattened, we can imagine an overall decrease in mobility of the ISJ, due possibly to a reduced muscle activity during the embryogenesis of these structures, as shown by Drachman & Sokoloff (1966) for chickens.

As there are no histological studies available for the condition of the ISJ in mammals other than humans, and in amniotes in general, drawing comparisons with other groups is rather difficult. Adaptation to a bipedal lifestyle in humans involved a great deal of evolutionary change in comparison to quadrupedal forms (Vleeming et al. 2012). The human sacrum is the result of the fusion of the three sacral vertebrae, and sometimes of the last lumbar vertebra (Fortin, 1993; Forst et al. 2006; Vleeming et al. 2012); the human ISJ is more typically formed between the first two sacral vertebrae and the ilia, and is considered a unique combination of a synarthrosis – dorsally, in correspondence with the first sacral vertebra – and a synovial joint – for the middle and ventral portion (Vleeming et al. 2012). Because of its composite nature, the mobility of the ISJ in humans has been highly debated in the literature, and not all authors agree on its full mobility or even on what type of movements are possible (Fortin, 1993; Forst et al. 2006; Rupert et al. 2009; Vleeming et al. 2012). The most recent interpretation of the ISJ in humans is that limited motion is possible in all three planes of the joint (i.e. frontal, transversal and sagittal), consisting essentially of a combined rotation–translation displacement (Vleeming et al. 2012). In comparison to humans, the ISJ of limbed squamates is far less complex, having only two sacral vertebrae contributing to form a single joint cavity for articulation with the ilium. At the macroscopic level, the overall configuration of the ISJ in crocodiles and most quadrupedal tetrapods seems to be similar to that of limbed lizards. However, this does not necessarily mean that the ISJ is similarly a synovial joint in these groups, something that will need to be further investigated through histological studies. As for birds and their highly specialized *bauplän*, the condition of the ISJ may well be more comparable to humans than to lizards considering that, in combination with their flying abilities, they are also adapted to a bipedal lifestyle. Birds are characterized by having a synsacrum, a structure that results from the fusion of vertebrae from the posterior thoracic, lumbar, sacral and occasionally caudal regions (Kardong, 2006). The synsacrum then fuses to the pelvic girdles, creating a single solid structure, implying that the nature of the ISJ in birds is likely synarthrotic. Again, in the absence of histological studies, a conclusive comparison of the ISJ across different amniote groups is unfortunately very limited at this point.

The joint between the two sacral ribs

The two sacral ribs in the specimens we analysed are distally sutured, to a greater or less extent depending on the different species. All our μCT-scanned specimens show a small gap at the confluence of sr-I and sr-II, excluding already the possibility of a synostosis (i.e. bone-to-bone contact; Figs 3; 5B; 7A–D; 8A–E). With our thin sections, we were able to determine that this space, however, is filled by dense fibres and no gap persists between the two bones (Fig. 5). As explained above, a fibrous-based contact is indicative of a syndesmosis, which allows for limited mobility (Barnett et al. 1961; Kardong, 2006). The presence of calcified cartilage, more distally along the margins of the sacral ribs, interposed between the subchondral bone and the fibres, suggests that this contact transitions to a synchondrosis towards the ISJ, similarly to what is described by Bailleul & Holliday (2017) for some cranial joints of modern alligators.

The cushioning properties of cartilage have been abundantly discussed in the literature (Martin et al. 1998a; Cormack, 2001; An & Martin, 2003; Hall, 2005; Levangie & Norkin, 2005; Bilezikian et al. 1996). Considering that our findings imply that the ISJ is fairly mobile, a non-rigid suture between the two sacral ribs may serve as a shock absorber (Martin et al. 1998b; Bilezikian et al. 1996). Moreover, limited translation in the transversal plane (perpendicularly to the vertebral column) cannot be excluded at least along the fibrous-only portion. However, we suspect that the nature of this contact may be more variable across limbed lizards, as previous studies have shown that during ontogeny the line of suture between the two sacral ribs can disappear completely in some taxa (e.g. geckos), with the two elements becoming fully fused to one another (Hoffstetter & Gasc, 1969). In this case, the joint between the two sacral ribs would certainly become immobile in older individuals.

Distinguishing between sacral ribs, diapophyses and lymphapophyses

One important issue regarding the homology of the elements involved in the ISJ system is represented by the confusion frequently found in the literature between sacral ribs and sacral transverse processes. In general, a vertebra can be defined as sacral when its rib mediates the contact between the vertebral column and the pelvic girdle (Romer, 1956; Hoffstetter & Gasc, 1969). The plesiomorphic number of sacrals in lizards is two, and both sacral vertebrae have distally expanded ribs bearing an articular surface at their tip. The undifferentiated use of 'sacral transverse processes' instead of 'sacral ribs' is incorrect as 'transverse process' (or diapophysis) should be limited to the projection from the vertebral neural arch that articulates with the rib tuberculum (one of the two heads of a rib: see Romer, 1956). Moreover, the ribs and transverse processes of the sacrals have two separate centres of ossification, meaning that in fact they are two separate elements (Winchester & Bellairs, 1977; Malashichev, 2001). A line of fusion between the transverse process proper and the ribs is usually visible early in ontogeny in most lizards while, in some groups of amniotes, such as ichthyosaurs and sauropterygians, the ribs never fuse to the vertebra (Romer, 1956; Motani et al. 1998; Malashichev, 2001; Cheng et al. 2004).

The sutured sacral ribs form what can be defined as a sacrum located between the two pelves (even though the two sacral vertebrae do not always fuse completely in lizards; Hoffstetter & Gasc, 1969). Our histological series of the *I. iguana* ISJ shows that the contact between the two sacral ribs is mostly fibrous-based, with some calcified cartilage found at the distal edges of the two bones (a syndesmotic-synchondrotic joint; Fig. 5). When the contact between the sacral vertebrae and the pelvic girdle is lost – as for instance in snakes – the distally expanded ribs do not bear an articular facet for an osseous contact with the ilium anymore, but in proximity of the pelvic elements it is usually possible to identify distally grooved or forked ribs for the support of the lymph hearts (i.e. cloacal vertebrae with lymphapophyses; Salle, 1880; Sood, 1948; Romer, 1956; Hoffstetter & Gasc, 1969; Woltering, 2012). We noticed that in some extant lizards, post-sacral vertebrae with distally grooved ribs can also be present: one in *V. albigularis* (UAMZ R947); two in *C. pallidus* (AMNH R-147848); and up to three in *Ctenosaura pectinata* (ROM R6709; Figs 11, 12). These grooved ribs likely are supporting the lymph hearts and should be considered homologous to the cloacal vertebrae in snakes. This would also suggest that the presence of vertebrae with lymphapophyses is independent from the presence/absence of sacral vertebrae. Interestingly, Malashichev (2001) shows in his study an anomalous specimen of *Lacerta vivipara*, with an asymmetry in the sacrals (and consequently in their contact with the ilium), where the right sacral ribs have shifted posteriorly by one vertebra. This results in the second sacral rib on the right side being paired with a left counterpart that is in fact distally forked, and not in contact with the ilium (i.e. a lymphapophysis). As was explained for the sacrals, the lymphapophyses are indeed ribs, and not elongated diapophyses, as they also have a separate centre of ossification, and only at some point during development do they fuse completely to the vertebral diapophyses (Malashichev, 2001).

In conclusion, sacral vertebrae in lizards can be defined as such if they possess all of the following features: (i) distally expanded ribs (fused to the diapophyses) converging to form a synovial cavity; (ii) consecutive ribs forming a sutural (synarthrotic) contact between the posterior/posteroventral distal end of the first sacral rib and the anterior/anteroventral distal end of the next sacral rib (a structure that can be defined as a sacrum); and (iii) ribs contacting the ilium via a synovial cavity.

Variability of the iliac processes and their implications for locomotion

Snyder (1954) analysed the anatomical differences between quadrupedal and facultative bipedal lizards, and recognized that bipeds have a narrower interacetabular width, a longer posterior process of the ilium, as well as a longer supracetabular process of the ilium. Moreover, in bipedal lizards there seems to be a greater distal fusion between the two sacral ribs, and the second sacral slopes forward favouring a more even distribution of the stress resulting from the body weight between the sacral vertebrae and the limb (Snyder, 1954). In addition to these aspects, we found that the following features also change across lizards with different locomotion habits: (i) the orientation of the posterior process of the ilium relative to the vertebral column from almost vertical to almost horizontal; and (ii) the shape of the supracetabular process – together with its length, as already emphasized by Snyder (1954) – from pointy and long (as in *Basiliscus* and *Pogona*: Figs 1C-E; 8H-I), to blunt and short (as in the marine iguana, *A. cristatus*: Fig. 10D-E), to basically absent (as in *Heloderma*: Fig. 9B, D).

Furthermore, we noted variation in the extent of the preacetabular process of the ilium, which is particularly long in taxa such as the extinct marine dolichosaurid *P. manduriensis* (Fig. 2A, D). However, the preacetabular process of the ilium extends ventrally to overlap onto the pubis head anteriorly, so that when the three pelvic bones fuse together its identity is blended with the anterior portion of the pubis, and thus it does not seem to have a specific function on its own. Considering that in terrestrial lizards this process becomes indiscernible when the ilium and pubis fuse completely, its relevance in terms of function is arguable, and this variation may be more related to phylogenetic relationships. For example, *P. manduriensis* is described as a semi-aquatic lizard in which the fusion of the pelvic bones is never complete during ontogeny (Paparella et al. 2018). In this case, a greatly extended preacetabular process may be a character shared with a terrestrial ancestor. A similar condition is also found in *Aigialosaurus dalmaticus* (Dutchak & Caldwell, 2006), and aigialosaurs and dolichosaurs are hypothesized to share a common ancestor (Lee & Caldwell, 2000; Caldwell, 2006; Conrad, 2008; Paparella et al. 2018). In fact, in obligatory aquatic forms such as mosasauroids, where the ilium, ischium and pubis do not fuse during ontogeny, the preacetabular process is either reduced or completely lost (IP personal observation; Bardet et al. 2003; Konishi et al. 2012; Makádi et al. 2012; Street & Caldwell, 2017; Jiménez-Huidobro et al. 2018).

Both posterior and supracetabular processes of the ilium play a role as muscle and ligament attachments. The supracetabular process of the ilium represents the site of attachment of the iliopubic ligament, and both the *musculus* (*m.*) *iliocostalis* and the *m. quadratus lumborum* also extend to this process, respectively, on its dorsal margin and medial surface (Snyder, 1954; Oldham & Smith, 1975). These muscles function to assist the *m. longissimus dorsi* in raising the trunk. From the dorsomedial side of the ilium, the *m. quadratus lumborum* attaches to the ventral surface of the sacral ribs, helping in stabilizing the spine and ribs (Snyder, 1954; Carrier, 1989; Moritz & Schilling, 2013). A longer supracetabular process means not only a longer surface for the attachment of these muscles, but also these muscles extending more anteriorly with respect to the rest of the body. This would likely have an effect on the centre of gravity of the body during locomotion, and thus being relevant to the possibility of a bipedal posture in some lizards, as described by Snyder (1954). The superficial *m. iliocaudalis dorsalis* and *m. iliocaudalis ventralis* anchor to the posterior process of the ilium, as well as the ilioischiadic ligament (Ali, 1948; Snyder, 1954; John, 1971). Both the *m. iliocaudalis dorsalis* and *ventralis* run posteriorly from the ilium, respectively, above and below the posterior surface of the sacral ribs and transverse processes of the caudal vertebrae, until the end of the tail. Their function is to abduct the tail, or stiffen the tail when contracted (Ali, 1948; John, 1971). The preacetabular process of the ilium, which extends ventrally to overlap onto the pubis head anteriorly, is not a primary surface of muscle or ligament attachment. Muscles such as the *m. puboischiofemoralis externus* and *m. puboischiofemoralis internus*, which anchor, respectively, to the lateral and medial side of the pubis, and are involved in the movements of the femur, can potentially reach up to the preacetabular process when the three pelvic bones are fused together (Snyder, 1954; Oldham & Smith, 1975). However, it is the development of the anterior process of the pubis that is most relevant to these muscles.

Movement at a joint occurs due to the action of muscles and ligaments on the skeletal elements. Previous embryological studies have shown that muscle movements are necessary to trigger the formation of synovial cavities (Carey, 1922; Drachman & Sokoloff, 1966). It is reasonable to assume that development of the ISJ as a synovial cavity in limbed lizards similarly happens early in ontogeny and the contact is then predisposed for mobility. Variations in the type of movements and arrangement of the muscles must have an effect in the growth and development of the joint systems throughout life. Limbed lizards can have either exclusively quadrupedal posture or also facultative bipedal posture (Snyder, 1954, 1962; Irschick & Jayne, 1999), and in both situations a series of joints between the appendicular and axial skeletons are involved during locomotion. The ISJ mobility must be highly dependent on the movements happening at the hip joint and involving the hindlimb in general. The modification of the bones as sites of soft tissue attachment is strongly indicative of variation in the locomotion habits of an animal. In forms such as *Amblyrhynchus* and *Heloderma*, with a semi-aquatic lifestyle, the use of limbs during swimming is limited, because they adopt an anguilliform style driven by lateral

undulations of the vertebral column. In this case, the axial musculature plays the most important role, and it makes sense that attachments for the appendicular musculature, like the iliopubic ligament that anchors to the supracetabular process of the ilium, undergoes reduction. At the same time, however, these animals still require a weight-bearing ISJ that allows them to keep moving on land, so the maintenance of this contact between the sacrum and the pelvic girdle remains necessary for efficient locomotion outside the water. This is consistent with the conclusions of Snyder (1954) that facultative bipedality in some iguanian lizards is related to the greater development of the supracetabular process, offering a larger site of attachment to the iliopubic ligament and appendicular musculature.

As seen above, the ISJ system is surrounded by both axial and appendicular muscles that are involved, respectively, in motion or stabilization of the trunk and tail, and various types of movements of the shank (Snyder, 1954, 1962; Oldham & Smith, 1975). In this framework, the mobility of the ISJ during locomotion can be a direct or indirect effect of the action of any of the associated muscles. We know that soft tissues (muscles and ligaments) are responsible for the development of joints (Carey, 1922; Drachman & Sokoloff, 1966), and we can assume that any rearrangement of those soft tissues can trigger anatomical variation of the structures involved with consequences on the type of possible movements, and hence locomotion style.

Conclusions

- At the osteological level, the elements involved in the ISJ (i.e. ilium and sacral ribs) across limb-bearing squamates display variability in a certain number of features. The iliac processes can vary in extension, cross-section and orientation in relation to the vertebral column, as well as to the other pelvic bones (pubis and ischium). The sacral ribs vary in the extension of their sutural contact, and their relative size and contribution to the joint cavity for the articulation with the ilium.
- The presence of a joint cavity (i.e. concave articular surface) formed by the convergence of the two sacral ribs is consistent across all the limb-bearing lizards analysed in this study. Histological analysis of the ISJ in *I. iguana* revealed this contact to be a synovial joint. The undivided cartilage cap that encompasses both sacral ribs makes clear that these two elements join together distally to form a single cavity for articulation with the posterior process of the ilium.
- As synovial joints develop in the embryo only if there is contraction of muscles, mobility seems to be a factor and not just a consequence for such structures. We hypothesize that the mobility of the ISJ in limbed lizards is tightly correlated to the movement of the hindlimb, and most likely limited to partial torsion (parallel to the vertebral column) of the ilium, together with absorption of the mechanical forces acting during compression and extension of the femur.
- The nature of the contact between the two sacral ribs is syndesmotic, or possibly a mix of a syndesmosis and a synchondrosis, being characterized by the presence of extensive collagen fibres holding the two bones together for most of the contact, with some calcified cartilage present on both elements more distally. Syndesmoses are contacts where limited mobility is allowed between the elements involved, and in the case of the two sacral ribs of limbed lizards we attribute to this joint a shock-absorbing function during locomotion.
- Muscles can increase as much as restrict the mobility at a joint, and in order to understand the changes in locomotory abilities that are consequential to the anatomical differences found in the ISJ apparatus, further research on the variation of the soft tissues is necessary.
- As histological analyses of the ISJ in other tetrapods are not currently available (except for humans), in order to understand if this joint as synovial is unique to squamates or rather common within Tetrapoda, a thorough study of this structure across the entire clade will need to be carried out.

Acknowledgements

For access to specimens, the authors are grateful to: Alison Murray and Braden Barr (UAMZ); Kevin Seymour and David Evans (ROM); Jolanta Kobylinska (ZPAL); Brandon Strilisky (TMP); Lauren Vonnahme, David Kizirian, Carl Mehling and Mark Norell (AMNH). For technical help and support during preparation and processing of samples, the authors are deeply thankful to Allan Lindoe, Arlene Oatway and Braden Barr. Insightful comments and suggestions by Alida Bailleul greatly improved this manuscript. Lastly, the authors thank the editorial team and in particular Edward Fenton for assistance. This research was funded in part by an NSERC Discovery Grant (#23458) and a University of Alberta, Faculty of Science, Chairs Research Allowance to MWC, and the Kay Ball Memorial Graduate Student Research Travel Award and Alberta Society of Professional Biologists Robin Leech Graduate Scholarship in Biological Sciences to IP.

Author contributions

IP and ARHL conceived the study, performed the histological analyses, and interpreted the data. MRD, IP and ARHL collected the CT-scan data. IP collected the osteological data, wrote the manuscript and prepared all the illustrations. ARHL and MRD contributed to the writing. MWC edited the manuscript. All authors provided critical revisions to the final draft.

REFERENCES

Ali S (1948) Studies on the anatomy of the tail in Sauria and Rhynchocephalia. Part II. *Chameleo zeylanicus*. *Proc Plant Sci* **28**, 151–165.

An YH, Martin KL, eds. (2003) *Handbook of Histology Methods for Bone and Cartilage*. Totowa: Humana Press.

Archer CW, Dowthwaite GP, Francis-West P (2003) Development of synovial joints. *Birth Defects Res C Embryo Today* **69**, 144–155.

Arnold P, Fischer MS, Nyakatura JA (2014) Soft tissue influence on *ex vivo* mobility in the hip of Iguana: comparison with *in vivo* movement and its bearing on joint motion of fossil sprawling tetrapods. *J Anat* **225**, 31–41.

Bailleul AM, Holliday CM (2017) Joint histology in *Alligator mississippiensis* challenges the identification of synovial joints in fossil archosaurs and inferences of cranial kinesis. *Proc Biol Sci* **284**. 20170038. The Royal Society.

Bardet N, Suberbiola XP, Jalil NE (2003) A new mosasauroid (Squamata) from the Late Cretaceous (Turonian) of Morocco. *CR Palevol* **2**, 607–616.

Barnett CH, Davies D, MacConaill M (1961) *Synovial Joints: Their Structure and Mechanics*. Springfield: Thomas.

Bejder L, Hall BK (2002) Limbs in whales and limblessness in other vertebrates: mechanisms of evolutionary and developmental transformation and loss. *Evol Dev* **4**, 445–458.

Bilezikian JP, Raisz LG, Rodan GA (1996) *Principles of Bone Biology*. Orlando: Academic Press.

Boisvert CA (2005) The pelvic fin and girdle of *Panderichthys* and the origin of tetrapod locomotion. *Nature* **438**, 1145–1147.

Borsuk-Białynicka M (2008) Evolution of the iliosacral joint in diapsid phylogeny. *Neues Jahrbuch für Geologie und Paläontologie - Abhandlungen* **249**, 297–311.

Caldwell MW (2006) A new species of *Pontosaurus* (Squamata, Pythonomorpha) from the Upper Cretaceous of Lebanon and a phylogenetic analysis of Pythonomorpha. *Memorie della Società Italiana di Scienze Naturali e Museo Civico di Storia Naturale di Milano* **34**, 1–43.

Caldwell MW, Palci A (2007) A new basal mosasauroid from the Cenomanian (U. Cretaceous) of Slovenia with a review of mosasauroid phylogeny and evolution. *J Vertebr Paleontol* **27**, 863–880.

Carey EJ (1922) Direct observations on the transformation of the mesenchyme in the thigh of the pig embryo (*Sus scrofa*), with especial reference to the genesis of the thigh muscles, of the knee- and hip-joints, and of the primary bone of the femur. *J Morphol* **37**, 1–77.

Carrier DR (1989) Ventilatory action of the hypaxial muscles of the lizard *Iguana iguana*: a function of slow muscle. *J Exp Biol* **143**, 435–457.

Carroll RL (1988) *Vertebrate Paleontology and Evolution*. New York: W. H. Freeman.

Carroll RL, Irwin J, Green DM (2005) Thermal physiology and the origin of terrestriality in vertebrates. *Zool J Linn Soc* **143**, 345–358.

Cheng YN, Wu XC, Ji Q (2004) Triassic marine reptiles gave birth to live young. *Nature* **432**, 383–386.

Coates MI, Jeffery JE, Ruta M (2002) Fins to limbs: what the fossils say. *Evol Dev* **4**, 390–401.

Conrad JL (2008) Phylogeny and systematics of Squamata (Reptilia) based on morphology. *Bull Am Mus Nat Hist* **310**, 1–182.

Cormack DH (2001) *Essential Histology*. Philadelphia: Lippincott Williams & Wilkins.

Drachman DB, Sokoloff L (1966) The role of movement in embryonic joint development. *Dev Biol* **14**, 401–420.

Dutchak AR, Caldwell MW (2006) Redescription of *Aigialosaurus dalmaticus* Kramberger, 1892, a Cenomanian mosasauroid lizard from Hvar Island, Croatia. *Can J Earth Sci* **43**, 1821–1834.

Forst SL, Wheeler MT, Fortin JD, et al. (2006) The sacroiliac joint: anatomy, physiology and clinical significance. *Pain Physician* **9**, 61–67.

Fortin JD (1993) Sacroiliac joint dysfunction. *J Back Musculoskelet Rehabil* **3**, 31–43.

Gans C, Gaunt A, Adler K (2008) *Biology of the Reptilia. Volume 21. Morphology I. The Skull and Appendicular Locomotor Apparatus of Lepidosauria*. Ithaca, New York: Society for the Study of Amphibians and Reptiles.

Gingerich PD, Raza SM, Arif M, et al. (1994) New whale from the Eocene of Pakistan and the origin of cetacean swimming. *Nature* **368**, 844–847.

Gray H (1878) *Anatomy of the Human Body*. Philadelphia: Lea & Febiber.

Hall BK (2005) *Bones and Cartilage: Developmental and Evolutionary Skeletal Biology*. New York: Academic Press, 792 pp.

Hoffstetter R, Gasc JP (1969) Vertebrae and ribs of modern reptiles. *Biology of the Reptilia* **1**, 201–310.

Irschick DJ, Jayne BC (1999) Comparative three-dimensional kinematics of the hindlimb for high-speed bipedal and quadrupedal locomotion of lizards. *J Exp Biol* **202**, 1047–1065.

Jiménez-Huidobro P, Caldwell MW, Paparella I, et al. (2018) A new species of tylosaurine mosasaur from the upper Campanian Bearpaw Formation of Saskatchewan, Canada. *J Syst Palaeontol* **17**, 849–864.

John KO (1971) Caudal musculature of the South Indian flying lizard *Draco dussumieri* Dum. and Bibr. *Acta Zoologica* **52**, 249–255.

Kardong KV (2006) *Vertebrates: comparative anatomy, function, evolution*. Boston: McGraw-Hill.

Konishi T, Lindgren J, Caldwell MW, et al. (2012) *Platecarpus tympaniticus* (Squamata, Mosasauridae): osteology of an exceptionally preserved specimen and its insights into the acquisition of a streamlined body shape in mosasaurs. *J Vertebr Paleontol* **32**, 1313–1327.

Lambert AE (1944) *Introduction and Guide to the Study of Histology*. Philadelphia: The Blankiston Company.

Lee MSY, Caldwell MW (2000) *Adriosaurus* and the affinities of mosasaurs, dolichosaurs and snakes. *J Paleontol* **74**, 915–937.

Levangie P, Norkin C (2005) *Joint Structure and Function: A Comprehensive Analysis*. Philadelphia: F.A. Davis Company.

Makádi L, Caldwell MW, Ősi A (2012) The first freshwater mosasauroid (Upper Cretaceous, Hungary) and a new clade of basal mosasauroids. *PLoS ONE* **7**, e51781.

Malashichev YB (2001) Sacrum and pelvic girdle development in Lacertidae. *Russ J Herpetol* **8**, 1–16.

Martin RB, Burr DB, Sharkey NA (1998a) *Skeletal Tissue Mechanics*. New York: Springer.

Martin RB, Burr DB, Sharkey NA, et al. (1998b) Synovial joint mechanics. In: *Skeletal Tissue Mechanics*, pp. 227–273. New York: Springer.

Moritz S, Schilling N (2013) Fiber-type composition in the perivertebral musculature of lizards: Implications for the evolution of the diapsid trunk muscles. *J Morphol* **274**, 294–306.

Motani R, Minoura N, Ando T (1998) Ichthyosaurian relationships illuminated by new primitive skeletons from Japan. *Nature* **393**, 255–257.

Oldham JC, Smith HM (1975) *Laboratory anatomy of the iguana*. Dubuque, Iowa: Wm. C. Brown.

Panzer S, Mc Coy MR, Hitzl W, et al. (2015) Checklist and scoring system for the assessment of soft tissue preservation in CT examinations of human mummies. *PLoS ONE* **10**, e0133364.

Paparella I, Palci A, Nicosia U, et al. (2018) A new fossil marine lizard with soft tissues from the Late Cretaceous of southern Italy. *R Soc Open Sci* **5**, 172 411.

Pierce SE, Clack JA, Hutchinson JR (2012) Three-dimensional limb joint mobility in the early tetrapod *Ichthyostega*. *Nature* **486**, 523–526.

Romer AS (1956) *Osteology of the Reptiles*. Chicago: University of Chicago Press.

Rupert M, Lee M, Manchikanti L, et al. (2009) Evaluation of sacroiliac joint interventions: a systematic appraisal of the literature. *Pain Physician* **12**, 399–418.

Salle O (1880) *Untersuchungen über die Lymphapophysen von Schlangen und schlangenähnlichen Sauriern*. Göttingen: Georg-August-Universität zu Göttingen.

Snyder RC (1954) The anatomy and function of the pelvic girdle and hindlimb in lizard locomotion. *Am J Anat* **95**, 1–45.

Snyder RC (1962) Adaptations for Bipedal Locomotion of Lizards. *Am Zool* **2**, 191–203.

Sood MS (1948) The anatomy of the vertebral column in serpentes. In *Proceedings of the Indian Academy of Sciences-Section B*, Vol. **28**, pp. 1-26. New Delhi: Springer India.

Street HP, Caldwell MW (2017) Rediagnosis and redescription of *Mosasaurus hoffmannii* (Squamata: Mosasauridae) and an assessment of species assigned to the genus *Mosasaurus*. *Geol Mag* **154**, 521–557.

Tsai HP, Holliday CM (2015) Articular soft tissue anatomy of the archosaur hip joint: structural homology and functional implications. *J Morphol* **276**, 601–630.

Tsai HP, Middleton KM, Hutchinson JR, et al. (2018) Hip joint articular soft tissues of non-dinosaurian Dinosauromorpha and early Dinosauria: evolutionary and biomechanical implications for Saurischia. *J Vertebr Paleontol* **38**, e1427593.

Vleeming A, Schuenke MD, Masi AT, et al. (2012) The sacroiliac joint: an overview of its anatomy, function and potential clinical implications. *J Anat* **221**, 537–567.

Winchester L, Bellairs AdA (1977) Aspects of vertebral development in lizards and snakes. *J Zool* **181**, 495–525.

Wolff HD (1990) Comments on the evolution of the sacroiliac joint. In: *Back Pain: An International Review* (eds Paterson JK, Burn L), pp. 175–185. Dordrecht, Netherlands: Springer.

Woltering JM (2012) From lizard to snake; behind the evolution of an extreme body plan. *Curr Genomics* **13**, 289–299.

Supporting Information

Additional Supporting Information may be found in the online version of this article:

Appendix S1. Masson's trichrome stain.